Brazilian Journal of Geology

REFERÊNCIA

DIAS, Tatiana Gonçalves et al. Age, provenance and tectonic setting of the high-grade Jequitinhonha Complex, Araçuaí Orogen, eastern Brazil. **Brazilian Journal of Geology**, São Paulo, v. 46, n. 2, p. 199-219, abr./jun. 2016. Disponível em: <http://www.scielo.br/scielo.php?script=sci_arttext&pid=S2317-48892016000200199&lng=en&nrm=iso>. Acesso em: 8 dez. 2017. doi: http://dx.doi.org/10.1590/2317-4889201620160012.

DOI: 10.1590/2317-4889201620160012

ARTICLE

Age, provenance and tectonic setting of the high-grade Jequitinhonha Complex, Araçuaí Orogen, eastern Brazil

Idade, proveniência e ambiente tectônico do Complexo Jequitinhonha de alto grau, Orógeno Araçuaí

Tatiana Gonçalves Dias[1]*, Fabrício de Andrade Caxito[1], Antônio Carlos Pedrosa-Soares[1], Ross Stevenson[2], Ivo Dussin[1], Luiz Carlos da Silva[3], Fernando Alkmim[4], Márcio Pimentel[5]

ABSTRACT: The Jequitinhonha Complex of the northeastern Araçuaí orogen is an extensive sedimentary unit metamorphosed in the amphibolite-granulite facies transition around 580–545 Ma. The unit consists of Al-rich (kinzigitic) paragneisses with decametric intercalations of graphite gneisses and quartzites, and centimetric to metric lenses of calcsilicate rocks. A new detrital zircon U-Pb age spectrum is reported for a sample of quartzite, and whole-rock geochemical (major and trace elements, 9 samples) and Sm-Nd isotope data (10 samples) for Jequitinhonha Complex paragneiss. Together with published data these show that: (1) the geochemistry of paragneiss samples of the Jequitinhonha Complex are similar to those of passive margin sedimentary protoliths; (2) detrital zircon data yield U-Pb age populations between ca. 0.9 and 2.5 Ga; and (3) Sm-Nd T_{DM} model ages range from 1.6 to 1.8 Ga and $\varepsilon Nd_{(575\ Ma)}$ around -7.5. The data reveal a mixture of Cryogenian to Mesoproterozoic rift-related igneous rocks with the Palaeoproterozoic-Archaean basement rocks of the São Francisco-Congo palaeocontinent as the main source areas, and also support the correlation between the Jequitinhonha Complex and the passive margin units of the upper Macaúbas Group, constituting the precursor basin of the orogen. Our results, with the absence of ophiolites in the Jequitinhonha Complex, reinforce the interpretation that the São Francisco-Congo palaeocontinent was not divided to the north of the focused region, suggesting an ensialic termination of a gulf during the Neoproterozoic.

KEYWORDS: Kinzigite gneiss; Jequitinhonha Complex; Araçuaí Orogen; West Gondwana.

RESUMO: *O Complexo Jequitinhonha é uma unidade sedimentar extensa da porção nordeste do orógeno Araçuaí, metamorfizada na transição entre as fácies anfibolito-granulito há cerca de 580–540 Ma. A unidade é composta por paragnaisses kinzigíticos com intercalações de grafita-gnaisse, quartzito e rochas calcissilicáticas. Dados U-Pb de zircão detrítico de uma amostra de quartzito e novos dados geoquímicos (nove amostras) e isotópicos (Sm-Nd) (dez amostras) são aqui apresentados. De maneira concomitante a dados previamente publicados, esses dados mostram que: (1) a geoquímica dos paragnaisses sugere uma afiliação do tipo margem passiva para as rochas metassedimentares; (2) zircões detríticos apresentam populações de idade U-Pb entre 0,9 e 2,5 Ga; e (3) dados isotópicos de Nd apresentam idades modelo T_{DM} entre 1,6 e 1,8 Ga e $\varepsilon Nd_{(575\ Ma)}$ ao redor de -7,5. Esses dados revelam uma mistura de fontes, envolvendo magmatismo de rift Criogeniano a Mesoproterozoico e o embasamento Paleoproterozoico-Arqueano do paleocontinente São Francisco-Congo, e sugerem uma forte correlação entre o Complexo Jequitinhonha e o Grupo Macaúbas, compondo a mais importante bacia precursora do orógeno Araçuaí. Além da natureza exclusivamente sedimentar do complexo, fatias ofiolíticas não foram encontradas na área, reforçando a interpretação da terminação ensiálica de um golfo e que o paleocontinente São Francisco-Congo não foi separado ao norte da região, agindo como uma única peça durante o Neoproterozoico.*

PALAVRAS-CHAVE: *Gnaisse kinzigítico; Complexo Jequitinhonha; Orógeno Araçuaí; Gondwana Ocidental.*

[1]Centro de Pesquisa Professor Manoel Teixeira da Costa, Programa de Pós-graduação em Geologia, Universidade Federal de Minas Gerais – CPMTC–IGC–UFMG, Belo Horizonte (MG), Brazil. E-mail: *tati_gdias@yahoo.com.br, facaxito@yahoo.com.br, pedrosa@igc.ufmg.br, ivodusin@yahoo.com.br*

[2]Département des Sciences de la Terre et de l'Atmosphère, GEOTOP, Université du Québec à Montréal, Montréal, Québec, Canada. E-mail: *stevenson.ross@uqam.ca*

[3]Geological Survey of Brazil, CPRM-SUREG-BH, Belo Horizonte (MG), Brazil. E-mail: l*uiz.silva@cprm.gov.br*

[4]Universidade Federal de Ouro Preto, Departamento de Geologia, Morro do Cruzeiro, Ouro Preto (MG), Brazil. E-mail: *alkmim@degeo.ufop.br*

[5]IG-Laboratório de Geocronologia, Universidade de Brasília, Asa Norte, Brasília (DF), Brazil. E-mail: *marcio@unb.br, marcio.pimentel@ufrgs.br*

*Corresponding author.

Manuscript ID: 20160012. **Received in:** 01/19/2016. **Approved in:** 04/15/2016.

INTRODUCTION

The process of West Gondwana assembly during the Neoproterozoic left significant sutural orogenic scars among the cratons of Brazil, resulting in the diachronous Brasiliano system of orogens (Trompette 1994, Brito Neves *et al.* 1999, Cordani *et al.* 2003). One example is the Araçuaí orogen (Pedrosa-Soares *et al.* 1992, 2008), bound by the eastern edge of the São Francisco craton (Almeida 1977) and the Atlantic continental margin (Fig. 1).

Prior to the opening of the South Atlantic Ocean, the Araçuaí orogen with its African counterpart, the West Congo belt (Fig. 1), constituted an important branch of the Brasiliano-Pan African orogenic system, surrounded on three sides by the São Francisco-Congo craton. This unusual configuration probably represented an inland-sea basin partially floored by oceanic crust, i.e. a gulf-like branch of the Adamastor Ocean (Pedrosa-Soares *et al.* 1998, 2001, Cordani *et al.* 2003, Alkmim *et al.* 2006). This configuration implies that the São Francisco-Congo palaeocontinent, assembled during the Rhyacian-Orosirian orogenies, was not completely disaggregated by Neoproterozoic rifting, but remained linked by a continental bridge (Fig. 1: the Bahia-Gabon bridge) at the northern end of the Araçuaí-West Congo orogenic system (e.g. Trompette 1994, Pedrosa-Soares *et al.* 2001, 2008, Alkmim *et al.* 2006, Noce *et al.* 2007).

This unique palaeogeographic interpretation has been checked by studies on the nature, age, and tectonic setting

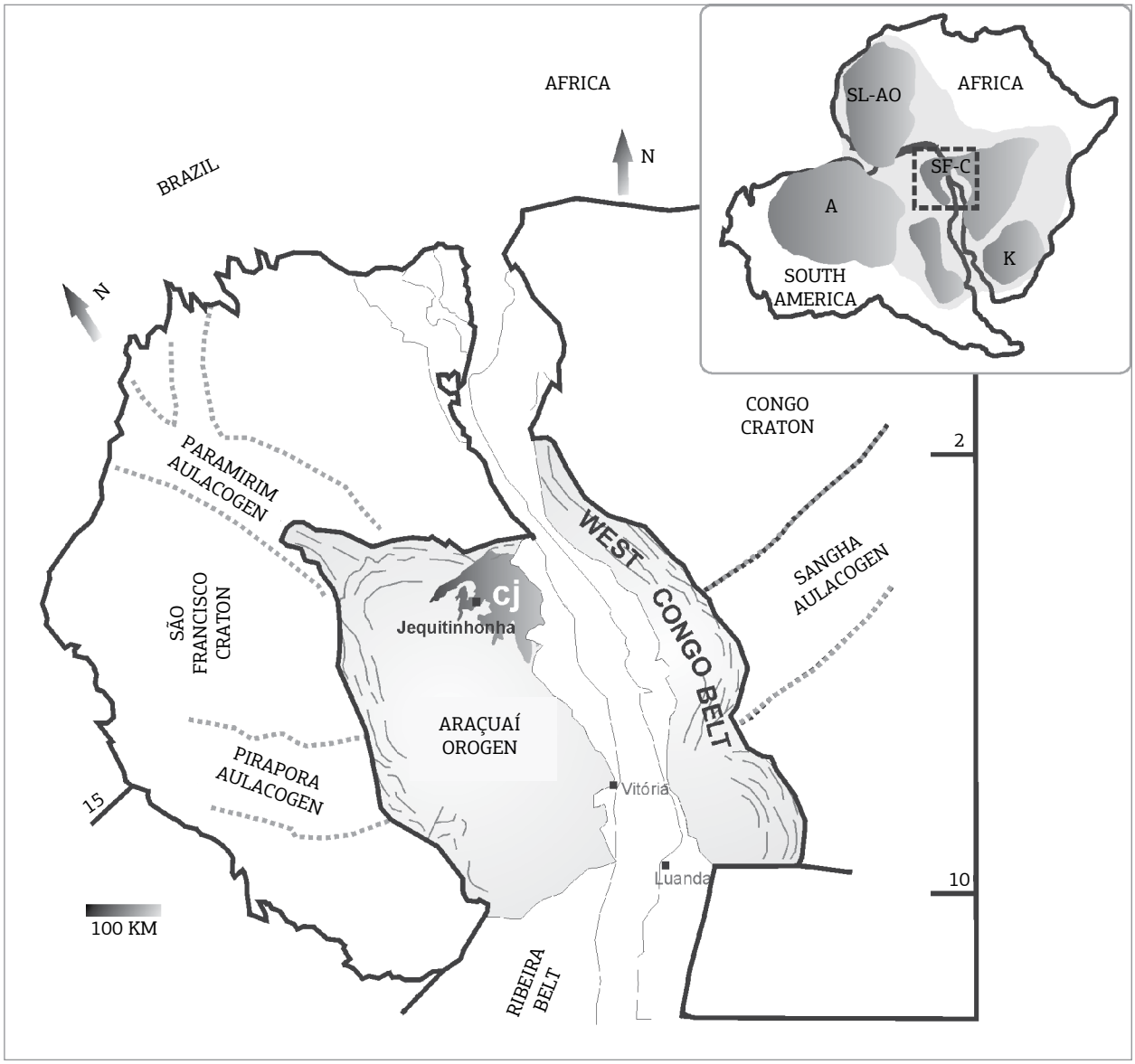

Figure 1. Geotectonic setting of the Jequitinhonha Complex (cj), located in the northeastern part of the Araçuaí Orogen (modified from Pedrosa-Soares *et al.* 2008).

of stratigraphic units located in the northern portion of the Araçuaí orogen. In this context, the Jequitinhonha Complex is a key unit represented by an extensive clastic sedimentary succession metamorphosed to the amphibolite-granulite facies (Fig. 1 and 2). In this work, we present new geochronological, field, petrographic, lithochemical, and isotopic data of the Jequitinhonha Complex type-area in order to characterize the age, depositional environment, provenance, and tectonic setting of this unit. Based on this dataset, we suggest a correlation of the Jequitinhonha Complex with the upper Macaúbas Group, representing the precursor basin of the Araçuaí orogen, and discuss its role in the evolution of the São Francisco – Congo paleocontinent.

GEOLOGICAL SETTING

The precursor basin to the Araçuaí Orogen is represented by the Macaúbas Group (Pedrosa-Soares *et al.* 2011b and references therein), an up to 10 km thick sedimentary unit that can be subdivided into three major sucessions: a pre-glacial sucession, composed by the Matão, Duas Barras, and

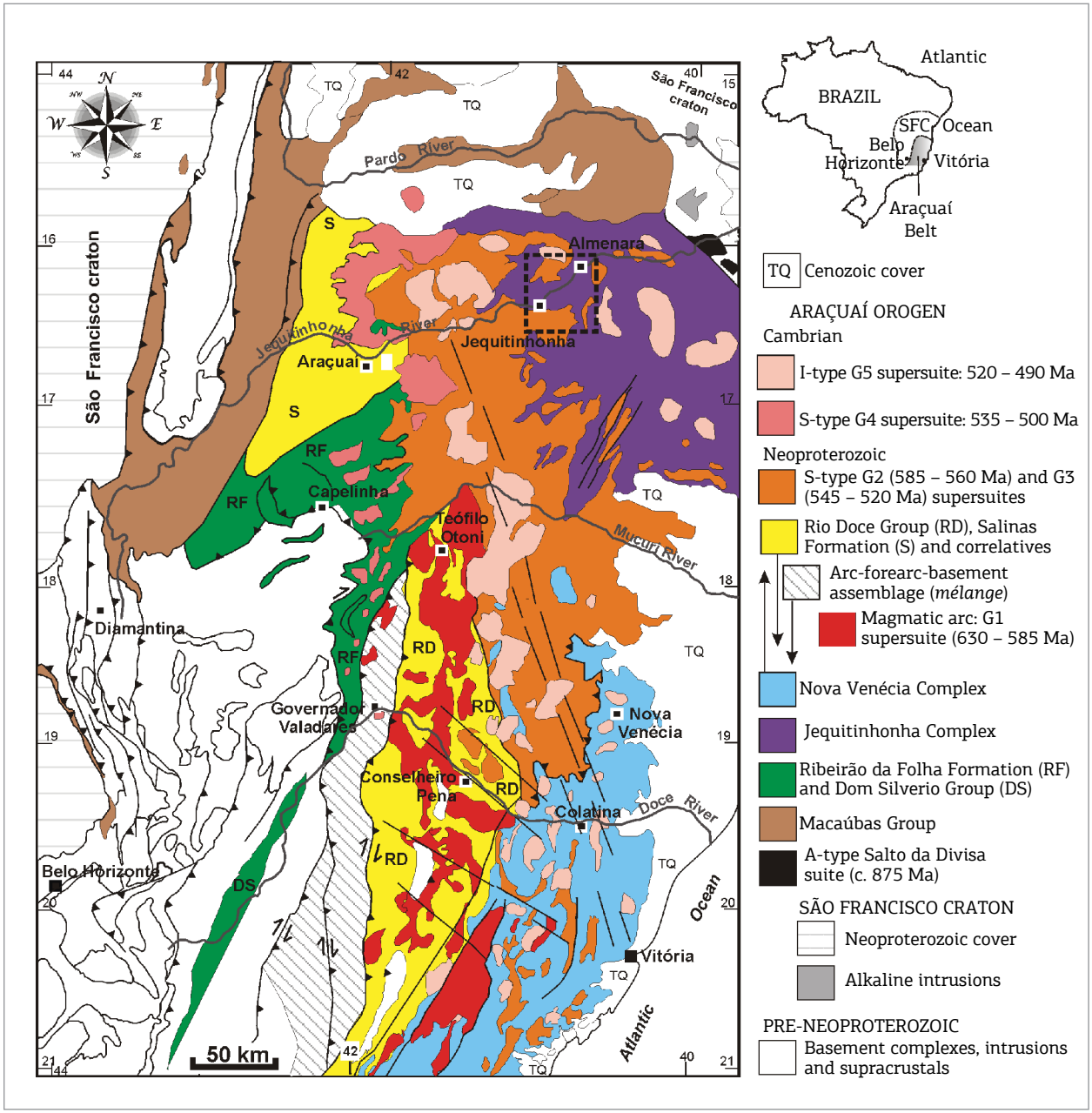

Figure 2. Geological map of the Araçuaí Orogen (modified from Pedrosa-Soares *et al.* 2007, 2008). The dashed rectangle shows the location presented in Figure 3.

Rio Peixe Bravo formations (quartzite, metaconglomerates and metabreccias); a glacial-related succession, composed of the diamictite-bearing Serra do Catuni, Nova Aurora, and Chapada Acauã formations; and a post-glacial sucession, composed of the diamictite-free Upper Chapada Acauã and Ribeirão da Folha succession, containing fine-grained turbidites and exhalites interleaved with metamafic and ultramafic rocks interpreted as remnants of a Neoproterozoic oceanic crust (Pedrosa-Soares *et al.* 1998, Queiroga *et al.* 2007).

Detrital zircon U-Pb data and the ages of related anorogenic igneous provinces suggest that deposition of the Macaúbas Group is related to at least three extensional events that took place during the Neoproterozoic (Pedrosa-Soares & Alkmim 2011): (i) a ca. 999 Ma event in the West Congo Belt; (ii) a ca. 930 – 870 Ma event which gave rise to continental rift basins (Zadinian and Mayumbian groups) and anorogenic magmatism of the Salto da Divisa granites and Pedro Lessa mafic dikes (Machado *et al.* 1989, Tack *et al.* 2001, Silva *et al.* 2008, Pedrosa-Soares *et al.* 2008, 2011a, Thiéblemont *et al.* 2011, Babinski *et al.* 2012); and (iii) a ca. 735 – 675 Ma continental rifting event (Rosa *et al.* 2007, Pedrosa-Soares *et al.* 2011a) that evolved to a passive margin setting with seafloor spreading, forming a confined oceanic basin, that is, a large gulf partially floored by oceanic crust. The post-glacial, diamictite-free units of the Macaúbas Group represent the infilling of this Cryogenian passive margin to ocean basin system (Pedrosa-Soares *et al.* 1998, 2001, 2008, 2011a, Queiroga *et al.* 2007).

Recently, Kuchenbecker *et al.* (2015) presented a comprehensive account of detrital zircon U-Pb data for various units of the Macaúbas Group. Overall, three main age peaks occur, at 900 – 1000 Ma, 1900 – 2200 Ma, and 2600 – 2800 Ma. The lack of Archaean zircons in the pre-glacial units and the relative abundance of Tonian zircons in the upper sequences demonstrate an important change in the source areas, coherent with the climate change to glacial conditions and the change of tectonic setting from rift-related to a passive margin basin.

Subsequently closure of the ocean basin generated calc-alkaline magmatism and eventual collision resulted in the Araçuaí orogen. Orogenic calc-alkaline magmatism started around 630 Ma and lasted until ca. 585 Ma in the core of the basin, building a pre-collisional magmatic arc represented by the G1 supersuite and volcano-sedimentary successions of the Rio Doce Group (Fig. 2) (Nalini *et al.* 2000, Pedrosa-Soares *et al.* 2001, 2011a; Martins *et al.* 2004, Vieira 2007, Paes *et al.* 2010, Silva *et al.* 2011). The Nova Venécia Complex, composed of peraluminous paragneiss with intercalations of calcsilicate rocks, represents pre-collisional deposition in the back-arc basin related to the G1 supersuite (Noce *et al.* 2004, Pedrosa-Soares *et al.* 2008, Gradim *et al.* 2014).

In addition to regional deformation and metamorphism, the syn-collisional stage generated a large volume of S-type granitic rocks, mostly represented by the biotite-garnet granite and two-mica granite of the G2 supersuite, dated at ca. 585 – 560 Ma (Pedrosa Soares *et al.* 2011a) (Fig. 2 and 3).

THE JEQUITINHONHA COMPLEX

The Jequitinhonha Complex was formerly defined by Almeida and Litwinski (1984) in the surroundings of Jequitinhonha and Almenara towns, northeastern Minas Gerais (Fig. 2 and 3). The unit mostly consists of paragneiss with thin intercalations of calcsilicate rock, lenses and layers of quartzite and graphite gneiss (Fig. 3 and 4). Metamorphic T-P conditions of 791 ± 42ºC at 5 ± 0.5 kbar were determined by multi-equilibrium thermobarometry (AvPT module in Thermocalc software, Powell & Holland 1994) using mineral chemistry data from a sillimanite-garnet-cordierite-biotite gneiss sampled close to Almenara (Belém 2006). These data, with the metamorphic mineral assemblages, indicate regional metamorphism in the amphibolite-granulite facies transition, accompanied by abundant partial melting of the kinzigitic gneiss (see also Uhlein *et al.* 1998). New multi-equilibrium thermobarometry data presented by Moraes *et al.* (2015) on migmatites and granulites correlative to the Jequitinhonha Complex in southern Bahia indicate metamorphic peak conditions of 850ºC and 7 kbar.

The first partial melting of the paragneiss produced biotite-garnet granite, locally rich in cordierite. This S-type granite underwent the regional deformation and represents the G2 supersuite (Pedrosa-Soares *et al.* 2011a). A second melting episode led to the generation of veins and patches of garnet-cordierite leucogranite free of the regional foliation, representing the G3 supersuite (Pedrosa-Soares *et al.* 2011a). Siga Jr. *et al.* (1987) presented a U-Pb (TIMS) age of late-stage zircon extracted from a kinzigitic gneiss sample, constraining the age of the main melting and metamorphic event at around 590 ± 20 Ma. This age overlaps with modern metamorphic ages found throughout the Araçuaí orogen that cluster around 575 Ma (Pedrosa-Soares *et al.* 2011a, Silva *et al.* 2011).

In the uppermost portion of the kinzigitic gneiss pile, an intercalated quartzite-rich unit up to 100 m thick forms a series of high plateaus and hills, in contrast to the lower smooth relief associated with the paragneiss. Paes *et al.* (2010) designated this quartzite layer as the Mata Escura Formation. We here consider this as a quartzite layer interleaved in the topmost portion of the paragneiss package, related to the other quartzite layers that occur within this package (Fig. 3).

MATERIALS AND METHODS

For geochemistry and isotopic analysis, only samples that include both the neosome and the paleosome of the gneisses were analysed, in order to obtain a full characterization of samples. For this, ca. 2 kg of each sample were crushed for analysis, and the fine powders obtained were thoroughly mixed before separation of a small fraction for geochemical analysis (ca. 300 g).

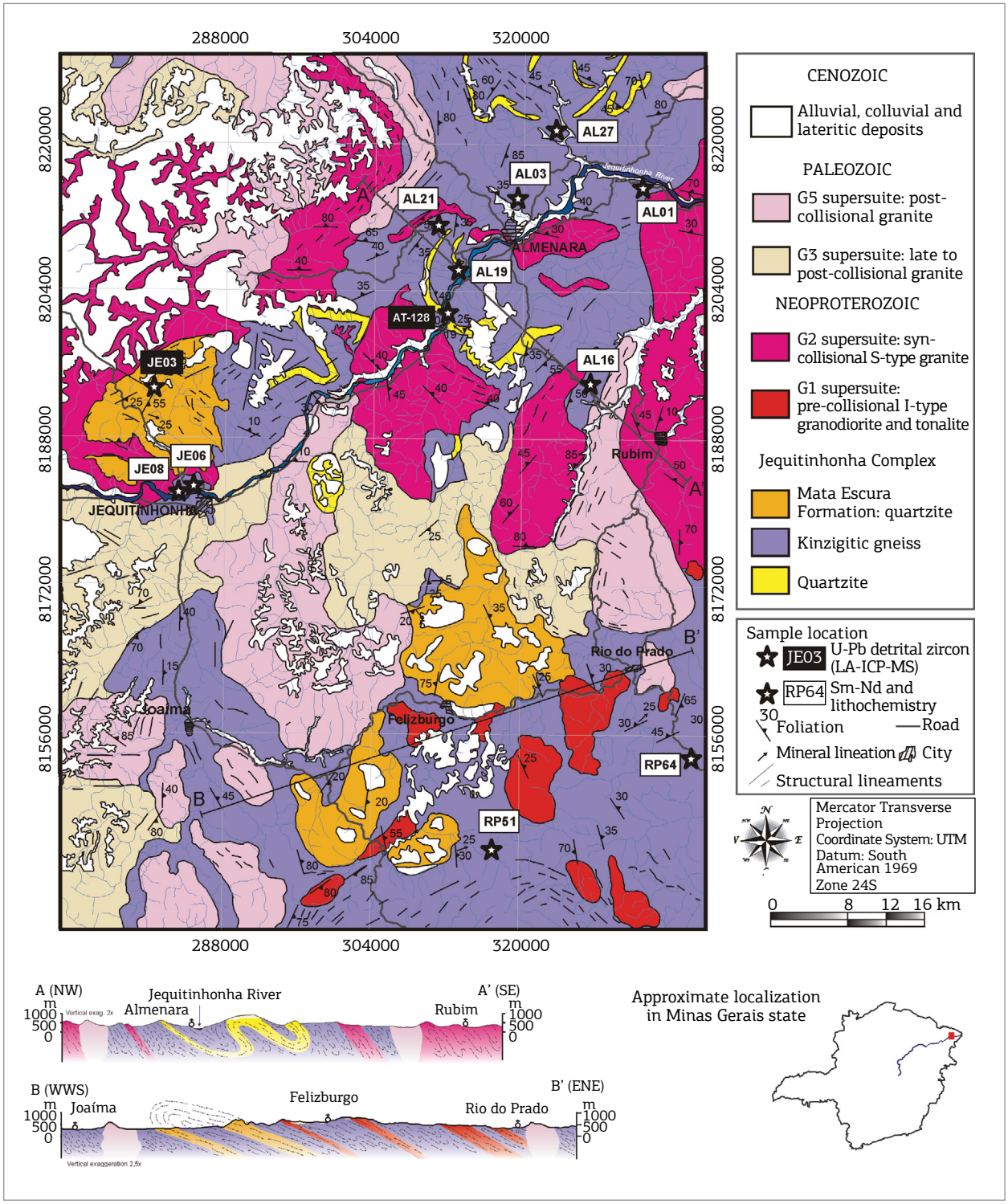

Figure 3. Geological map and sections of the Almenara-Jequitinhonha region, northeastern Minas Gerais State, showing the location of the analysed samples. The map is partially compiled from Drumond & Malouf (2010), Gomes (2010), Junqueira *et al.* (2010), and Pinto (2010).

Whole-rock geochemical analysis of nine paragneiss samples was conducted at the ACME Analytical Laboratories Ltd., Vancouver, Canada, via ICP-MS, with 5 % precision for oxides and 10 – 15% for most of the trace and rare earth elements.

The Sm-Nd isotopic analyses were conducted at the GEOTOP Research Center, Université du Québec à Montréal, Canada, on a ThermoScientific Triton Plus Mass Spectrometer operating in static mode, using both the JNdi standard and USGS standard BHVO-2 as control. The Sm and Nd concentrations and the ^{147}Sm / ^{144}Nd ratios have an reproducibility of 0.5% that corresponds to an average error on the initial εNd value of ± 0.5. For details on the methodology used in the geochemical and Sm-Nd analysis, see Caxito *et al.* (2015).

For the zircon U-Pb analysis, 10 kg of a quartzite sample from the Mata Escura Formation (JE03) was crushed in carefully cleaned equipment, and grains were separated through standard magnetic and hand-picking techniques. Morphological features and internal structures of zircon grains were revealed by electron backscattered electron (BSE) and cathodoluminescence (CL) images. Analyses were conducted at the Research School of Earth Sciences, The Australian National University, in a Neptune Multicollector Inductively Coupled Plasma Mass Spectrometer (MC-ICP-MS). Results were corrected for common lead content using the ^{204}Pb / ^{206}Pb ratio. For the full U-Pb analytical procedures followed in this study and machine parameters, see Kuchenbecker *et al.* (2015).

RESULTS

The Jequitinhonha Complex in the studied area

Peraluminous paragneiss is the most common gneiss variety in the studied area, typically banded and showing distinct migmatite structures owing to different degrees of partial melting (Fig. 4A and 4B). In addition to quartz and feldspars (plagioclase > K-feldspar), the blueish grey paleosome is rich in biotite, cordierite, garnet and/or sillimanite (Fig. 4C and 4D), with traces of graphite, resembling the so-called kinzigite sensu strictu (Mehnert 1971). The neosome includes the granitic leucosome and a quartz-feldspar poor melanosome to mesosome variably rich in biotite, garnet and/or cordierite. In fact, the paragneiss is a rock assemblage, called by the general name "kinzigitic gneiss", derived from a sedimentary series with variable contributions of clay minerals and carbonaceous material, now composed of sillimanite-graphite gneiss (whose protolith was the richest in carbonaceous material and iron-free clay), graphite-sillimanite-garnet-cordierite-biotite gneiss (richest protolith in clay fraction and the most abundant variety), garnet-cordierite-biotite gneiss, garnet-biotite gneiss, and biotite gneiss (poorest protolith in clay minerals, but the richest in sand fraction). These gneisses show different degrees of partial melting and preserve migmatite features, such as ptigmatic, stromatic, augen, schollen, and schlieren structures (Fig. 4). Centimetric to metric lenses of calcsilicate rocks, intercalated within the paragneiss, consist of quartz, plagioclase, microcline, light pink (Ca-rich) garnet, clinopyroxene and orthopyroxene, and represent mud-carbonate (marl) sediment.

The kinzigitic gneiss package also includes thin lenses to thick layers of quartzite (quartz sandstone), feldspathic quartzite, and sillimanite-graphite-biotite quartzite that grades to the paragneiss. The quartzite typically shows a coarse-grained sacaroidal texture and massive to foliated structure (Fig. 4E and 4F).

Lithochemistry

New major and trace element analyses of 9 paragneiss samples (Tab. 1) are compared with data presented by Reis (1999), Teixeira (2002), Daconti (2004), and Paes *et al.* (2010), totalling 35 paragneiss samples that spatially represent the varieties of this rock in the Jequitinhonha Complex (Fig. 5 and 6). Samples of the Macaúbas Group schists that crop out nearby (Teixeira 2002) are also plotted for comparison.

Regionally, the paragneiss samples show a wide range of Al_2O_3 (11.49 – 19.80%) reflecting the relative abundance of peraluminous silicates (biotite, cordierite, garnet and/or sillimanite), that is, the clay fraction in the protolith, as so the silica contents (57.82 – 75.93%) in relation to the abudance of sand (quartz + feldspars). K_2O (0.24 – 4.93%) compared to Na_2O (0.87 – 3.24%) and CaO (0.33 – 6.85%) contents, together with modal contents from thin sections (biotite up to 35%, plagioclase up to 30%, K-feldspar up to 10%), point to the predominance of the phyllosilicates and plagioclase over K-feldspar.

The bivariant diagrams for major and trace elements (Fig. 5 and 6) show decreasing trends of Al_2O_3, TiO_2 and MgO relative to SiO_2, and increasing MgO, TiO_2, Cr, and V relative to Al_2O_3, reflecting variable mixtures of clay-size (phyllosilicate) and sand (quartz-feldspar) fractions in the protoliths. Al, Ti, Mg, Cr and V are preferentially concentrated in the clay minerals of mud deposits. Trends of increasing MgO and V in relation to Al_2O_3 reflect the original sedimentary composition. The decrease of K_2O and the corresponding increase of Al_2O_3 relative to silica suggest the preferential absorption of potassium by clay minerals, in contrast to the contribution of clastic K-feldspar. This interpretation is also supported by the decrease of Na_2O + CaO as K_2O increases, i.e, most sodium and calcium was provided

by the sand fraction (probably clastic plagioclase and carbonate), but most potassium was provided by the mud contribution. TiO_2 variation relative to silica suggests a similar interpretation, that is, most titanium is incorporated in the mud fraction, rather than in heavy minerals in the sand fraction.

Higher Na_2O + CaO and Sr + Ba in comparison to K_2O and Rb contents characterize most paragneiss located along

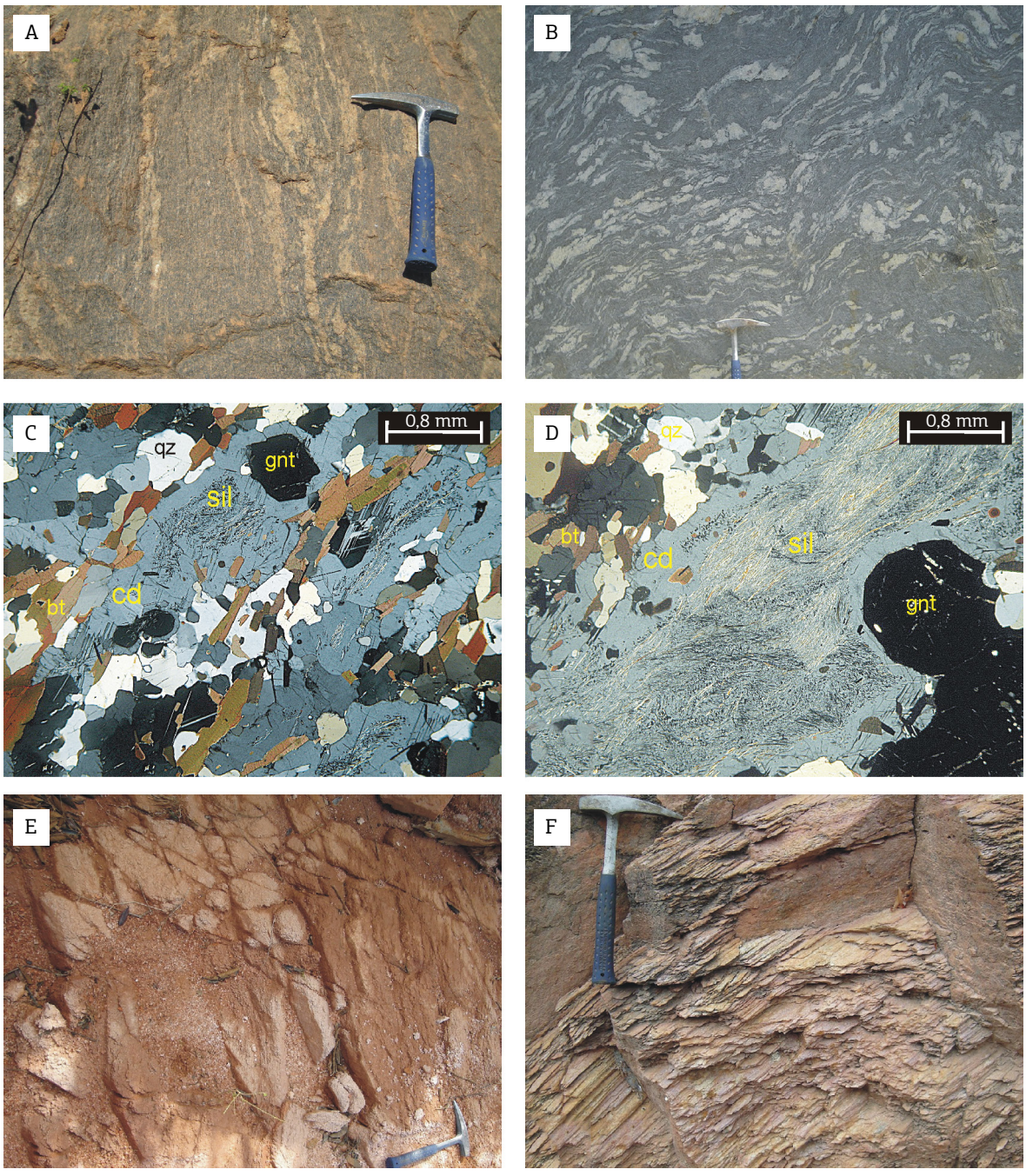

Figure 4. Petrographic features of rocks from the Jequitinhonha Complex. (A) Typical banded kinzigitic paragneiss. (B) Folded migmatite with dark grey kinzigitic paleosome and vein-shaped granitic leucosome. (C) Photomicrograph of kinzigitic gneiss under crossed polars, showing the regional foliation (qz: quartz; bt: biotite; cd: cordierite; gnt: garnet; sil: sillimanite); (D) Photomicrograph of kinzigitic gneiss under crossed polars, highlighting a peraluminous band composed of cordierite poikiloblasts (cd) with fibrous sillimanite (sil) roughly oriented along the regional foliation, intergrown with garnet (gnt). (E) Foliated, coarse-grained, sacaroidal quartzite of the Mata Escura Formation. (F) Medium- to coarse-grained quartzite intercalated in the kinigitic gneiss package.

Table 1. Lithochemistry data from paragneiss samples of the Jequitinhonha Complex.

Sample	AL01	AL27	AL21	AL03	RP64	JE08	RP51	JE06	AL16A
UTM coord.	335405 /8215547	322357/ 8226222	310029/ 8211137	318673/ 8213968	340509/ 8152465	285271/ 8182872	315062/ 8144209	285390/ 8182951	327292/ 8194091
Major elements (wt %)									
SiO_2	58.47	58.50	58.94	59.72	59.90	60.45	61.30	64.13	73.69
TiO_2	1.07	1.00	1.12	1.02	1.04	1.01	1.06	0.96	0.80
Al_2O_3	19.06	18.95	17.59	17.95	17.67	17.94	17.93	16.24	11.49
Fe_2O_3	9.83	9.96	10.31	10.12	7.93	9.03	9.03	7.69	5.56
MnO	0.16	0.15	0.15	0.18	0.10	0.14	0.11	0.13	0.09
MgO	4.00	4.15	4.19	3.52	3.67	3.60	3.73	3.02	1.75
CaO	0.72	0.66	0.71	0.48	2.28	0.69	0.59	0.87	1.19
Na_2O	1.60	1.46	1.63	1.46	2.86	1.75	1.51	2.12	2.55
K_2O	4.05	3.94	3.97	4.26	2.53	3.53	3.33	3.24	2.09
P_2O_5	0.09	0.11	0.07	0.10	0.17	0.13	0.09	0.15	0.08
Cr_2O_3	0.019	0.019	0.019	0.034	0.015	0.016	0.017	0.014	0.011
LOI	0.7	0.9	1.1	0.8	1.6	1.5	1.1	1.3	0.6
TOT/C	0.10	0.12	0.14	0.08	0.19	0.15	0.05	0.11	0.07
TOT/S	0.06	0.04	0.07	0.06	0.16	<0.02	0.22	<0.02	0.09
Sum	99.76	99.79	99.78	99.65	99.78	99.78	99.79	99.84	99.92
Trace elements (ppm)									
Ba	625	548	557	702	482	639	529	382	147
Rb	191.1	199.2	196.8	194.0	188.9	194.3	143.6	199.0	176.7
Sr	100.4	86.2	126.7	79.7	201.0	83.8	77.2	80.7	89.0
Cs	6.3	5.4	6.5	6.7	7.1	10.8	5.6	9.2	9.1
Tl	0.5	0.9	1.1	0.9	0.9	1.0	0.5	1.0	0.9
Ta	0.8	0.8	1.2	2.7	2.0	1.1	1.0	1.4	1.7
Nb	18.1	14.3	19.7	20.9	44.1	15.6	16.6	17.8	23.1
Hf	6.2	5.0	5.7	6.1	5.4	5.4	5.9	6.7	5.7
Zr	200.3	169.0	192.7	208.3	183.1	187.3	206.3	211.0	212.7
Y	34.6	31.2	30.7	34.1	22.3	32.2	33.4	33.5	14.3
Th	17.3	14.1	14.0	15.2	16.2	15.1	15.3	15.0	11.5
U	2.8	2.5	2.8	4.4	3.5	3.3	3.2	4.0	3.9
Co	27.7	22.8	22.2	163.4	19.2	21.8	23.1	18.5	11.1
Sc	24	24	24	25	15	20	19	17	13
V	211	164	171	184	156	158	166	135	94
Cu	47.9	29.8	23.0	30.3	37.1	34.7	84.6	11.7	19.5
Pb	1.3	1.2	2.0	1.4	2.0	1.5	1.4	1.3	1.9
Zn	111	112	139	123	141	105	100	94	97

Continue...

Table 1. Continuation.

Sample	AL01	AL27	AL21	AL03	RP64	JE08	RP51	JE06	AL16A
UTM coord.	335405 /8215547	322357/ 8226222	310029/ 8211137	318673/ 8213968	340509/ 8152465	285271/ 8182872	315062/ 8144209	285390/ 8182951	327292/ 8194091
Bi	<0.1	<0.1	<0.1	0.2	<0.1	0.4	<0.1	0.6	0.2
Be	1	<1	2	2	4	2	2	2	1
Ga	25.6	23.7	25.7	26.1	29.3	24.7	23.5	20.5	18.7
Sn	<1	2	2	1	1	3	1	3	3
W	<0.5	<0.5	<0.5	828.2	0.6	0.7	<0.5	<0.5	0.6
As	<0.5	<0.5	<0.5	<0.5	<0.5	<0.5	<0.5	<0.5	<0.5
Au	0.9	0.6	0.6	<0.5	<0.5	<0.5	<0.5	0.6	2.1
Mo	0.6	0.4	0.6	3.8	0.5	0.4	0.5	0.3	0.5
Ni	63.0	60.6	58.3	59.2	47.0	55.0	56.4	45.2	27.9
Th/Sc	0.72	0.59	0.58	0.61	1.08	0.76	0.81	0.88	0.88
Rare earth elements (ppm)									
La	40.4	36.7	39.3	41.5	39.5	38.1	40.1	38.7	22.4
Ce	91.3	77.4	82.5	97.4	86.8	86.7	92.7	88.8	47.5
Pr	9.89	8.88	9.44	10.19	9.07	9.33	9.72	9.57	5.52
Nd	37.0	34.7	36.2	38.1	34.0	34.8	37.8	36.0	20.1
Sm	7.10	6.30	6.48	7.33	6.07	6.79	7.17	7.21	3.44
Eu	1.49	1.30	1.04	1.38	1.10	1.29	1.36	1.26	0.78
Gd	6.25	5.63	5.70	6.68	5.32	6.25	6.59	6.44	2.55
Tb	1.05	0.96	0.94	1.07	0.82	1.04	1.06	1.08	0.43
Dy	5.68	5.13	5.00	6.00	4.40	5.76	5.66	6.02	2.14
Ho	1.20	1.10	1.06	1.24	0.81	1.12	1.16	1.18	0.48
Er	3.63	3.29	3.38	4.00	2.11	3.40	3.28	3.44	1.76
Tm	0.55	0.52	0.54	0.61	0.33	0.52	0.50	0.54	0.33
Yb	3.49	3.32	3.62	3.92	1.97	3.27	3.20	3.30	2.41
Lu	0.54	0.51	0.52	0.58	0.30	0.50	0.48	0.50	0.38
ΣREE	209.57	185.74	195.72	220.00	192.60	198.87	210.78	204.04	110.22
La_N/Yb_N	8.3	7.9	7.8	7.6	14.4	8.4	8.9	8.4	6.7
Eu/Eu*	0.7	0.7	0.5	0.6	0.6	0.6	0.6	0.6	0.8

the northern to eastern border of the complex, where silica contents are also high, reflecting the predominance of plagioclase over K-feldspar and even less abundant biotite. In general, relatively high SiO_2 / Al_2O_3 and low K_2O / Na_2O ratios suggest sand-mud protoliths richer in plagioclase than in K-feldspar.

McLennan *et al.* (1990) pointed out that the Th / Sc ratio is a sensitive indicator of sediment provenance, because Th is highly incompatible whereas Sc is relatively compatible, so that it can be used as an indicator of the predominance of continental versus juvenile sources. The Th / Sc ratio of the paragneiss samples varies from 0.6 to 1.1 (Tab. 1), similar to trailing edge (i.e., passive plate margin) sediments (0.73 – 1.4), but quite distinct from those of juvenile arc-related sediments (0.003 – 0.7; Fig. 7) or the high values (up to 1.8) of continental arc basins (Taylor & McLennan 1985).

Chondrite-normalized rare earth elements (REE) patterns of the paragneiss are moderately enriched in light rare earth elements (LREE) (La_N / Yb_N = 6.7 – 14.4) and show prominent negative Eu anomalies (Eu / Eu* = 0.5 – 0.8; Fig. 8A), compatible with modern passive margin turbidite muds (La_N / Yb_N = 4.4 – 13.6; Eu / Eu* = 0.58 – 0.75; McLennan *et al.* 1990). In contrast, sediments from arc-related basins typically show lower enrichments of LREE and less prominent negative Eu anomalies (La_N / Yb_N = 2.09 – 11.7; Eu / Eu* = 0.7 – 0.96; McLennan *et al.* 1990), reflecting erosion of less fractionated sources. The rare earth element contents of the Jequitinhonha samples are very similar to NASC, showing a flat NASC-normalized pattern (Fig. 8B; Grommet *et al.* 1984). The only exceptions are sample RP64, which shows slight heavy rare earth element (HREE) depletion, probably owing to trapping of HREE in garnet; and sample AL16A, which is the richest in quartz so that the total amount of REE is lower than in the other samples. The REE patterns of other gneiss samples from the same region (Paes *et al.* 2010; La_N / Yb_N = 6.6 – 11.4, Eu / Eu* = 0.4 – 0.8) are very similar to the new data presented here.

U-Pb (LA-ICP-MS) data

U-Pb analysis of detrital zircon from one quartzite sample of the Jequitinhonha Complex (AT-128) was formerly presented by Gonçalves-Dias *et al.* (2011). Another sample (JE-03) from the uppermost thick quartzite (Mata Escura Formation) NNW of Jequitinhonha city was analysed (Fig. 3, Fig. 9, and Fig. 10). Results are displayed in a histogram and also in a probability density plot calculated using the *Isoplot 3.6* software (Ludwig 2008).

A total of 52 zircon grains were recovered and analysed from sample JE03. Most of these grains are well-rounded to sub-rounded, but some of them show subhedral shapes, ranging in size from 100 to 450 µm. Oscillatory zoning is also a common feature (Fig. 9). From these 52 zircons, 49 analysed spots in the same namber of zircons yielded concordant data (< 10% discordance; Tab. 2). Most Th / U values range from

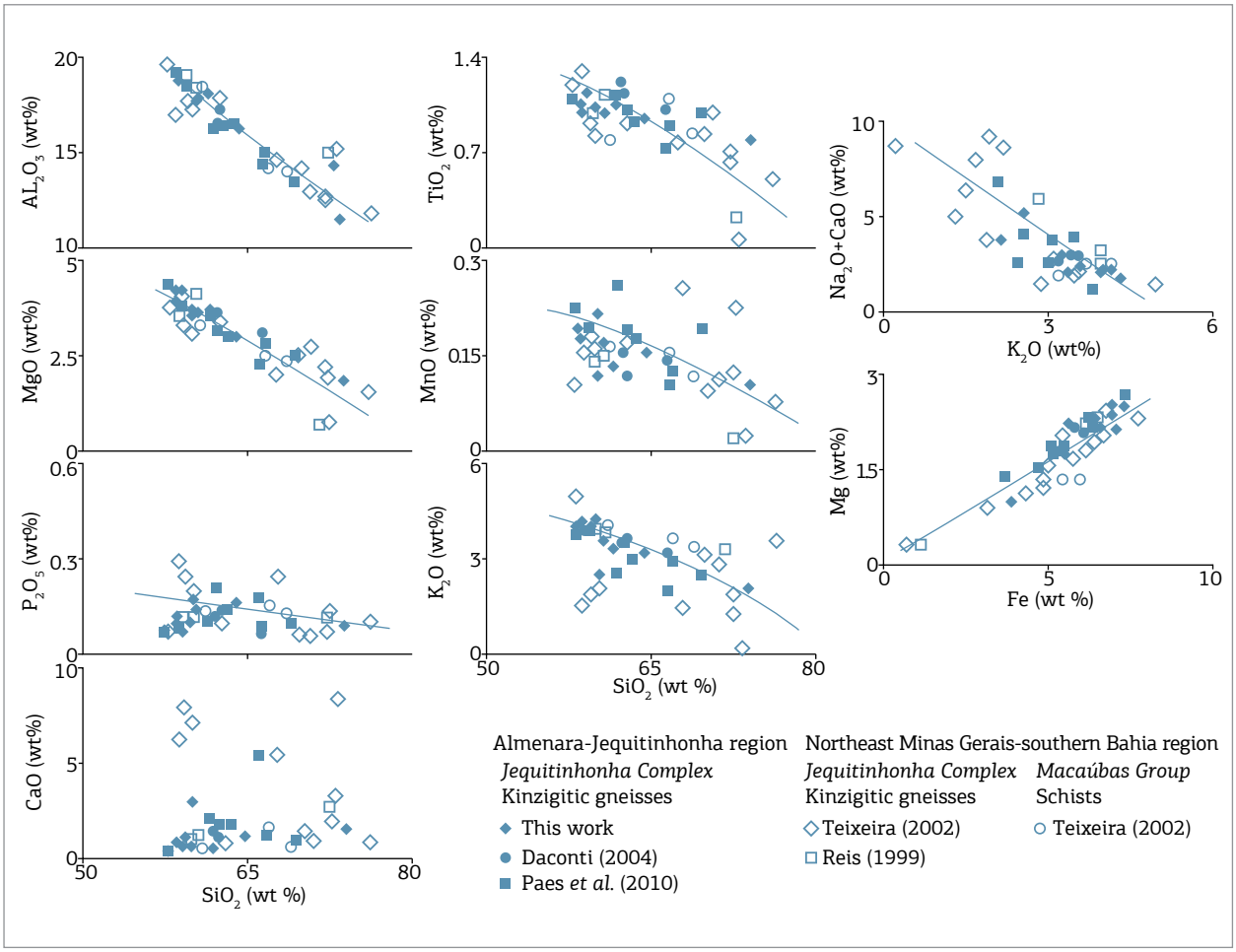

Figure 5. Major element bivariant diagrams for kinzigitic gneiss samples from different parts of the Jequitinhonha Complex, compared with schist samples of the Macaúbas Group.

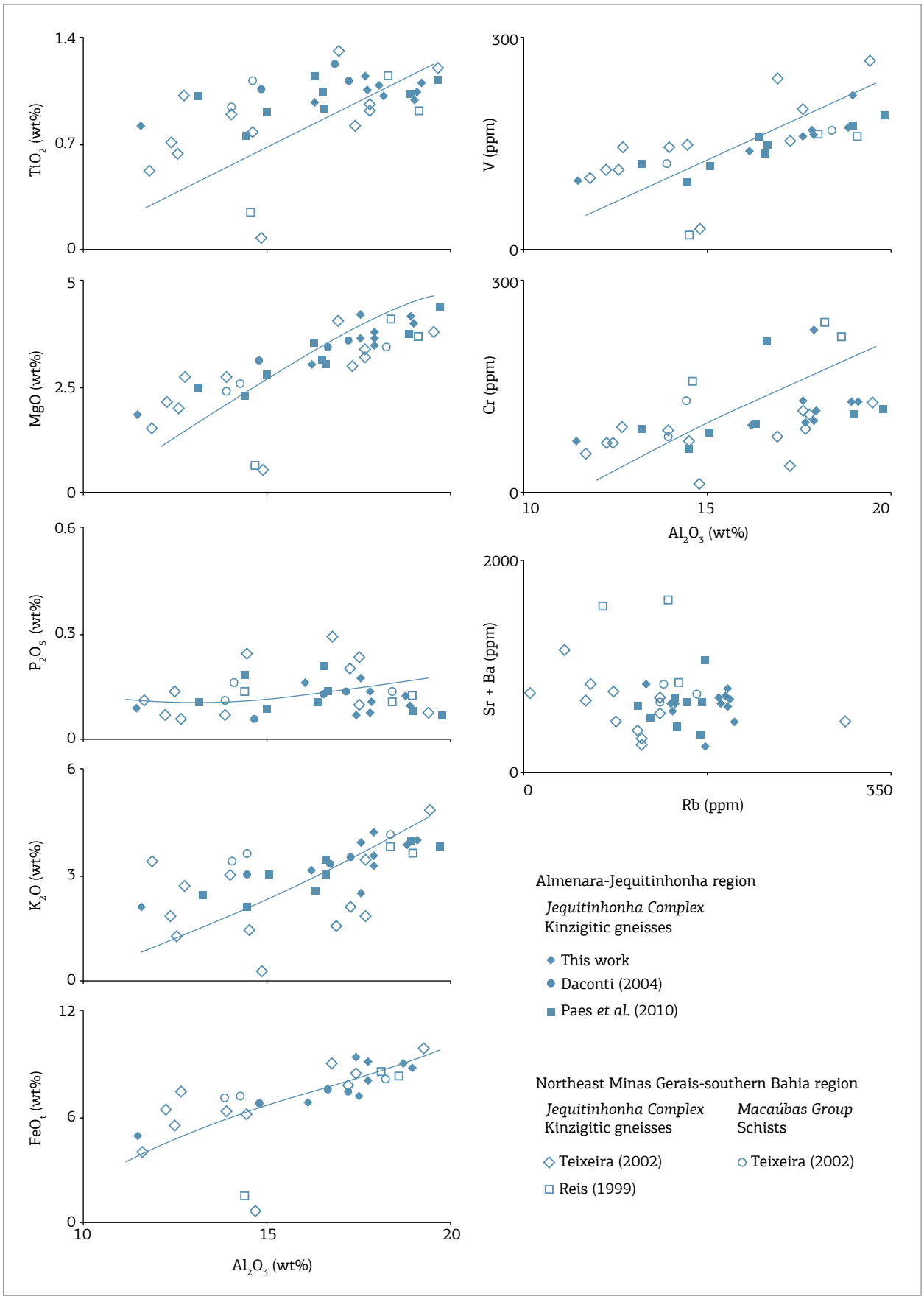

Figure 6. Major and trace element bivariant diagrams for kinzigitic gneiss samples from different parts of the Jequitinhonha omplex, compared with schist samples of the Macaúbas Group.

0.2 to 1.4, with some reaching up to 3.2, and are consistent with a magmatic origin for these zircon grains. The concordant analyses yielded a ^{207}Pb / ^{206}Pb age spectrum with five main peaks (Fig. 10) at ca. 1.0, 1.2, 1.5, 1.8, and 2.2 Ga. The age of the youngest concordant zircon grain is 916 ± 24 Ma (spot number 58.D), with 98% concordance (Table 2).

These results are similar to those published for sample AT-128 (Gonçalves-Dias *et al.* 2011), which yielded a ^{207}Pb / ^{206}Pb age spectrum with six main peaks at 1.0, 1.2, 1.5, 1.8, 2.0, and 2.5 Ga (Fig. 11). The main difference between the two samples is the minor Archean peak, which is absent in sample JE-03.

Sm-Nd data

Nd isotopic data were obtained for nine paragneiss and one quartzite sample (Table 3). The initial isotope ratios were recalculated to 575 Ma, which is the main age of the metamorphic peak in the Araçuaí orogen (Pedrosa-Soares *et al.* 2011a). The paragneiss samples yield a very homogeneous Nd isotopic signature, with ^{143}Nd / ^{144}Nd ratios from 0.511919 to 0.511980, $\varepsilon Nd_{(575\ Ma)}$ around -7.5 and T_{DM} model ages (De Paolo 1981) from 1.6 Ga to 1.8 Ga. Sm / Nd ratios in the range of 0.18 – 0.20 are typical of the upper continental crust (Faure 1986).

Sample AT-128, a quartzite layer interleaved within paragneiss, clearly shows an isotopic bias toward older sources,

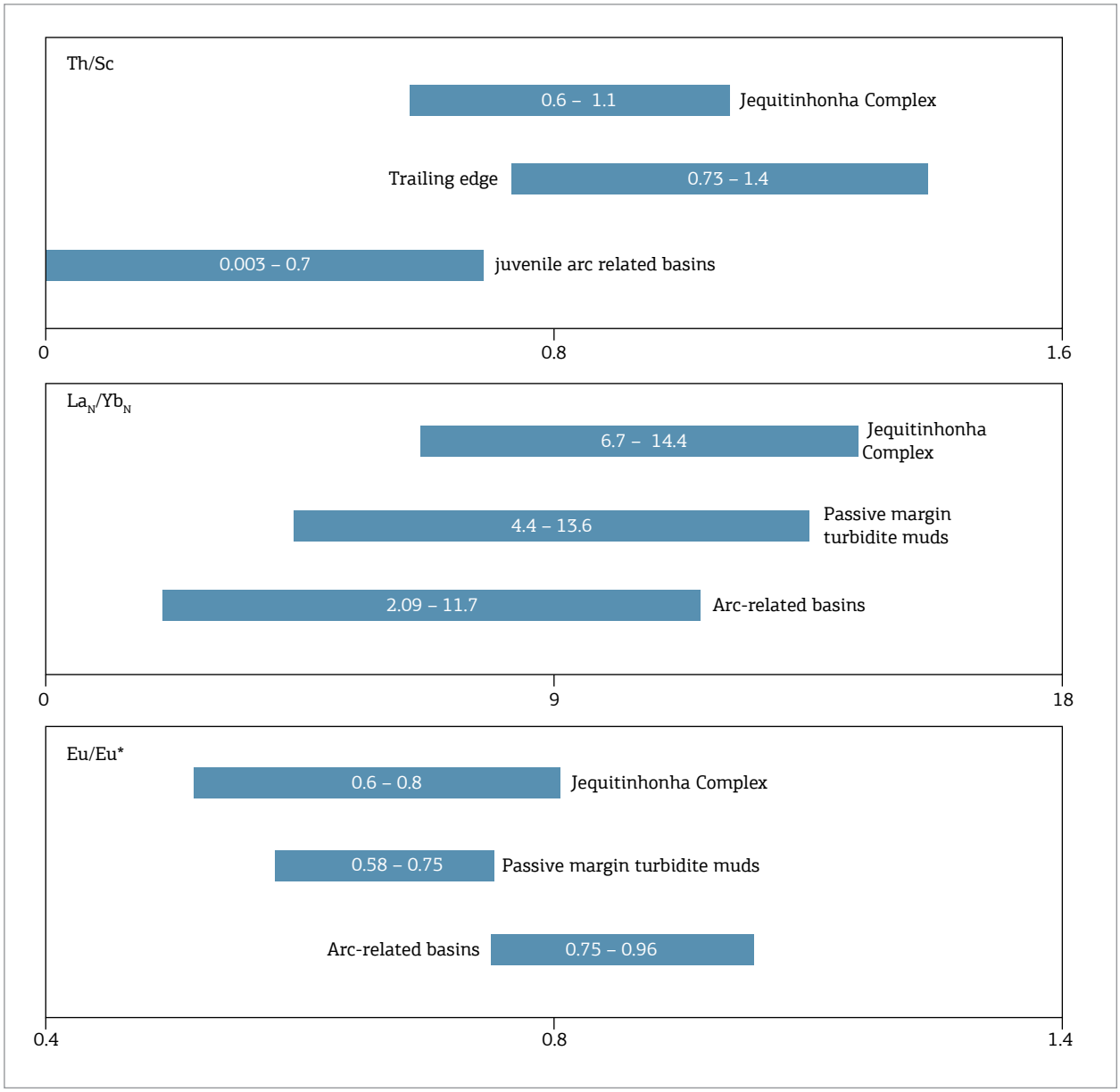

Figure 7. Patterns of trace and rare earth elements of the Jequitinhonha Complex: Th / Sc values compared to those of trailing edge and juvenile arc-related sediments (Taylor & McLennan 1985), and La_N / Yb_N and Eu / Eu* values compared to passive margin turbidite muds and arc-related basins patterns (McLennan *et al.* 1990).

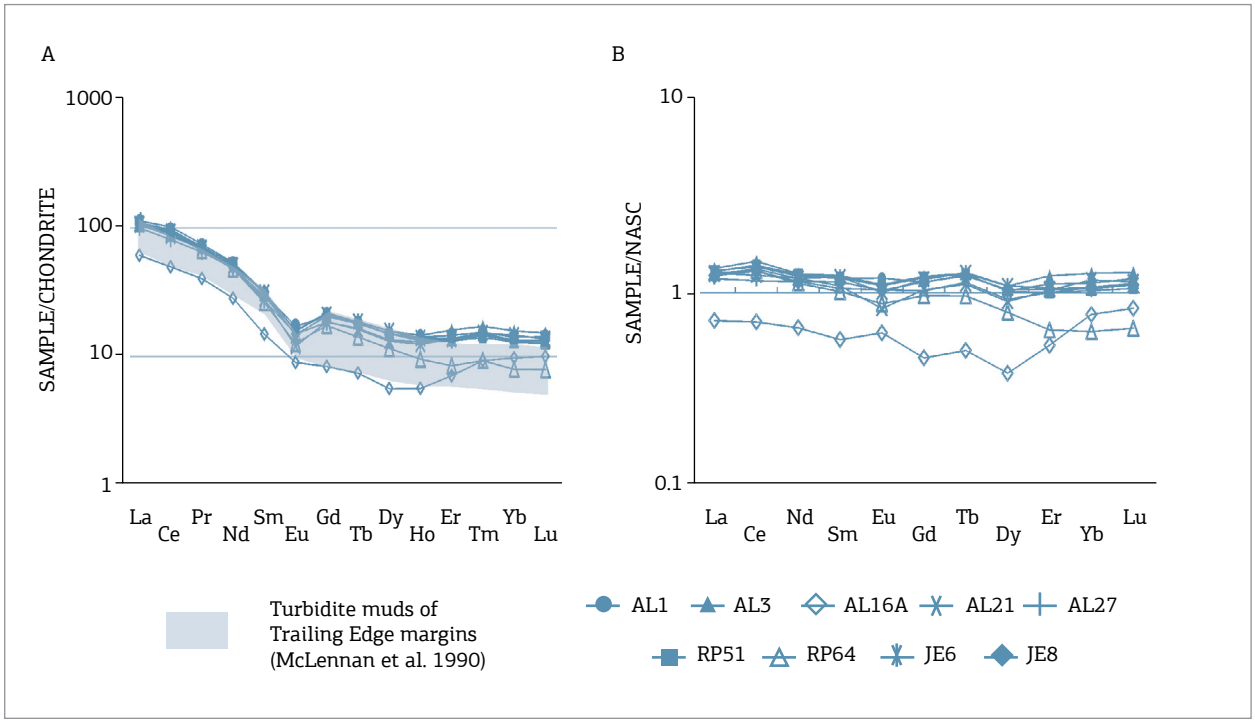

Figure 8. Rare earth elements patterns for paragneiss samples from the Jequitinhonha Complex. (a) Chondrite-normalized diagram (Taylor & McLennan 1985), with a shaded field representing turbidite muds from trailing edge margins (McLennan *et al.* 1990); (b) NASC-normalized diagram (Grommet *et al.* 1984).

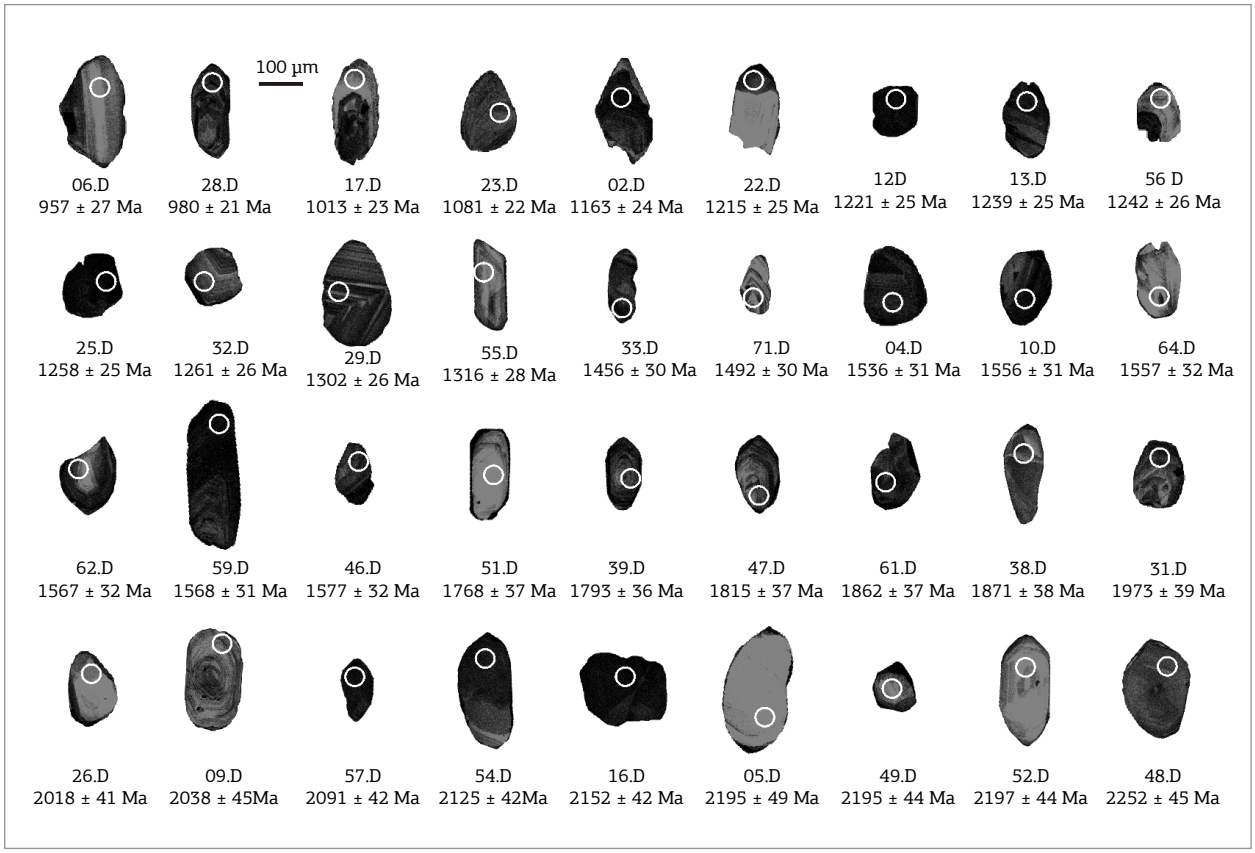

Figure 9. Selected cathodoluminoscence images and spot placement for zircons of sample JE03.

with T_{DM} = 2.4 Ga, and $\varepsilon Nd_{(575\ Ma)}$ = -17.9. Fine-grained and/or clay-rich sediments are more likely to represent large and distant source regions, whereas coarse-grained rocks can be biased towards specific nearby source areas (Frost & Winston 1987, Evans *et al.* 1991).

Celino (1999) also presented Sm-Nd data for the Jequitinhonha Complex. Four paragneiss samples (one of them is a xenolith within a syn-collisional granite) yielded similar T_{DM} model ages (1.6 – 1.7 Ga). Daconti (2004) also presented results from two paragneiss samples collected in the surroundings of Almenara region, which yielded quite similar T_{DM} model ages to ours (1.76 Ga and 1.83 Ga).

DISCUSSION

Sedimentary Provenance

Excluding the few Archaean zircon grains of sample AT-128 (Fig. 11), the two quartzite samples of the Jequitinhonha Complex (JE-03 and AT128) show very similar age spectra, with main age peaks in the ca. 1.0, 1.2, 1.5, 1.8, and 2.15 Ga, with a minor Archean peak. Potential sources for the Archaean and Palaeoproterozoic zircon grains are common in the basement of São Francisco-Congo craton and in the basement of the Araçuaí-West Congo orogen (e.g. Teixeira *et al.* 2000, Silva *et al.* 2002, Barbosa & Sabaté 2004, Noce *et al.* 2007). The Espinhaço-Chapada Diamantina basin system developed upon the São Francisco craton and associated magmatism are the most probable Statherian and Mesoproterozoic sources (e.g. Danderfer *et al.* 2009, Pedrosa-Soares & Alkmim 2011, Chemale *et al.* 2012). The youngest zircon population can be assigned to the A-type magmatism of the Tonian precursor basin of the orogen, representing erosion of rift shoulders and internal horsts in the cratonic margin bordering the northern and eastern Araçuaí orogen (e.g. Tack *et al.* 2001, Silva *et al.* 2008, Pedrosa-Soares & Alkmim 2011).

Figure 11 shows a comparison of the detrital zircon age spectra of the two analysed samples and samples from the upper Macaúbas Group (upper Chapada Acauã Formation and Ribeirão da Folha Formation), which are considered to represent the distal passive margin of the precursor basin to the Araçuaí Orogen, and also a comparison with samples from the Nova Venécia Complex paragnaisses and the Rio Doce Group, which are believed to represent syn-orogenic basins related to the erosion of the G1 magmatic arc (Noce *et al.* 2004, Pedrosa-Soares *et al.* 2000, 2011a, Gonçalves-Dias *et al.* 2011, Novo 2013, Gradim *et al.* 2014, Peixoto *et al.* 2015, Kuchenbecker *et al.* 2015).

Despite some differences, such as the relative abundance of Archean detrital zircons in the Upper Chapada Acauã Formation and the peak of 1.2 Ga zircons in the Jequitinhonha Complex, the range of detrital zircon ages of the Jequitinhonha Complex is more similar to those of the upper units of the Macaúbas Group. In particular, both the Jequitinhonha Complex and the upper Macaúbas Group samples lack the distinctive Cryogenian – Ediacaran peak found in samples of metasedimentary units related to the G1 magmatic arc (Rio Doce Group and Nova Venécia Complex).

The younger detrital zircon populations of the Jequitinhonha Complex samples constrain the maximum

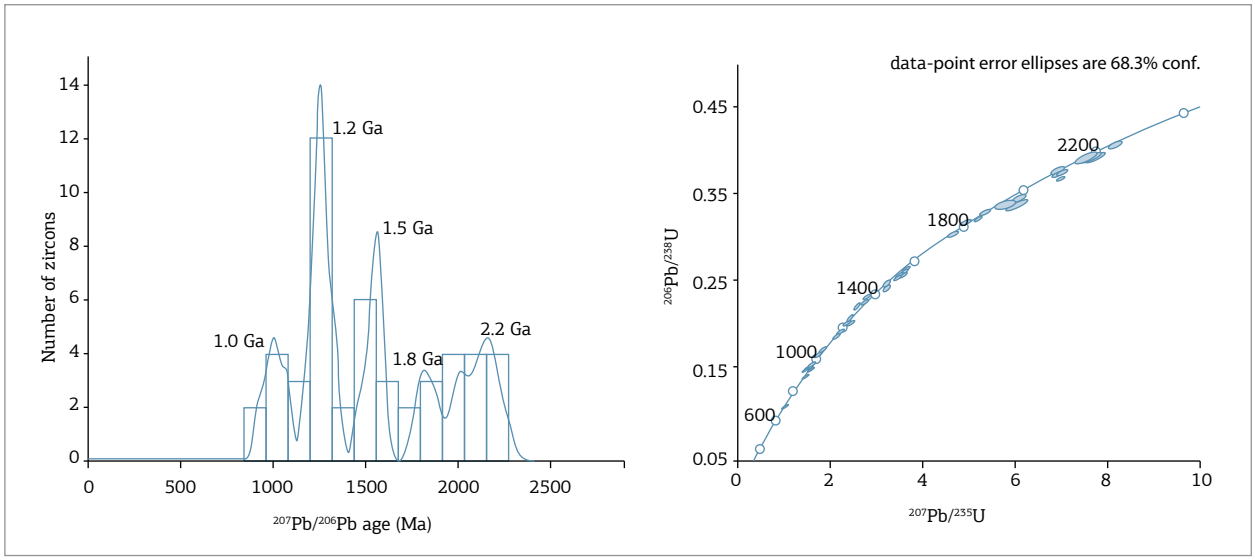

Figure 10. Age histogram, probability density plot and Wetherill concordia diagram for U-Pb data from detrital zircon grains from sample JE-03.

Table 2. U-Pb (LA-ICP-MS) data for detrital zircon grains from quartzite sample (JE-03) from the Mata Escura Formation of the Jequitinhonha Complex. Shaded rows highlight more than 10% discordant data.

Spot	U (ppm)	Th/U	Pb (ppm)	$f^{206}Pb$ (%)	Ratios							Ages						
					$^{206}Pb/^{238}U$	± 1σ	$^{207}Pb/^{235}U$	± 1σ	$^{207}Pb/^{206}Pb$	± 1σ	ρ	$^{206}Pb/^{238}U$	±	$^{207}Pb/^{235}U$	±	$^{207}Pb/^{206}Pb$	±	Disc. (%)
02.D	337.1	0.53	70.0	0.0015	0.1923	0.56	2.0851	1.12	0.07862	0.97	0.80	1134	23	1144	24	1163	24	2
04.D	204.2	0.32	55.5	0.0021	0.2633	0.52	3.4631	0.94	0.09541	0.78	0.79	1506	30	1519	31	1536	31	2
05.D	39.0	0.39	17.0	0.0023	0.4017	1.06	7.6121	2.82	0.13742	2.61	0.74	2177	47	2186	50	2195	49	1
06.D	46.6	0.65	8.3	0.0000	0.1600	0.89	1.5664	3.20	0.07099	3.08	0.74	957	20	957	27	957	27	0
09.D	89.5	0.55	34.5	0.0118	0.3479	1.27	6.0257	2.72	0.12564	2.41	0.70	1924	43	1980	45	2038	45	6
10.D	354.2	0.33	97.6	0.0022	0.2669	0.51	3.5475	0.90	0.09642	0.74	0.79	1525	31	1538	31	1556	31	2
11.D	49.9	0.52	8.8	0.0062	0.1653	0.84	1.7495	2.29	0.07677	2.13	0.79	986	21	1027	25	1115	26	12
12.D	381.5	0.49	83.5	0.0011	0.2048	0.43	2.2872	0.97	0.08099	0.87	0.78	1201	24	1208	25	1221	25	2
13.D	391.8	0.50	97.0	0.0000	0.2298	0.81	2.5892	1.28	0.08171	1.00	0.80	1334	28	1298	27	1239	25	-8
14.D	230.2	0.53	57.4	0.0000	0.2300	0.59	2.7174	1.15	0.08568	0.99	0.80	1335	27	1333	27	1331	27	0
15.D	41.8	0.58	18.1	0.0033	0.3831	0.80	6.9485	1.54	0.13155	1.31	0.80	2091	43	2105	43	2119	43	1
16.D	359.6	0.31	143.5	0.0101	0.3777	0.48	6.9818	0.72	0.13407	0.54	0.78	2065	41	2109	42	2152	42	4
17.D	93.2	0.45	16.0	0.0017	0.1636	0.81	1.6459	1.98	0.07299	1.80	0.80	977	20	988	23	1013	23	4
20.D	135.8	0.39	28.9	0.0036	0.2047	0.68	2.3389	1.65	0.08288	1.50	0.80	1200	25	1224	27	1266	27	5
21.D	350.8	0.26	69.0	0.0024	0.1957	0.50	2.1589	1.01	0.08002	0.88	0.79	1152	23	1168	24	1197	24	4
22.D	180.6	0.28	36.5	0.0022	0.1997	0.50	2.2231	1.21	0.08074	1.10	0.79	1174	24	1188	25	1215	25	3
23.D	173.1	0.34	32.0	0.0007	0.1800	0.62	1.8733	1.18	0.07548	1.00	0.80	1067	22	1072	22	1081	22	1
25.D	466.7	0.26	94.9	0.0038	0.2023	0.71	2.3010	1.14	0.08251	0.90	0.80	1187	24	1213	25	1258	25	6
26.D	46.6	1.25	21.3	0.0066	0.3542	0.85	6.0673	1.56	0.12425	1.31	0.80	1954	41	1986	41	2018	41	3
28.D	173.5	0.62	28.0	0.0036	0.1496	0.60	1.4813	1.58	0.07181	1.47	0.80	899	18	923	20	980	21	8
29.D	168.0	0.74	40.8	0.0035	0.2123	0.61	2.4714	1.13	0.08442	0.95	0.80	1241	25	1264	26	1302	26	5
30.D	149.6	0.76	26.2	0.0053	0.1567	0.51	1.6087	1.35	0.07446	1.25	0.80	938	19	974	21	1054	22	11
31.D	168.1	0.75	67.7	0.0056	0.3466	0.56	5.7900	0.94	0.12117	0.79	0.79	1918	38	1945	39	1973	39	3
32.D	103.7	0.61	24.1	0.0016	0.2108	0.63	2.4028	1.45	0.08267	1.31	0.80	1233	25	1243	26	1261	26	2
33.D	292.0	0.58	82.3	0.0000	0.2561	0.65	3.2292	1.27	0.09144	1.10	0.80	1470	30	1464	30	1456	30	-1
38.D	87.8	1.10	37.6	0.0000	0.3397	0.63	5.3580	1.33	0.11440	1.17	0.80	1885	38	1878	38	1871	38	-1
39.D	120.2	0.88	47.0	0.0000	0.3265	0.65	4.9358	1.19	0.10963	0.99	0.80	1821	37	1808	37	1793	36	-2
42.D	30.1	2.84	17.6	0.0058	0.3483	1.10	5.8537	3.33	0.12188	3.14	0.71	1927	42	1954	48	1984	47	3
46.D	188.2	0.63	56.2	0.0037	0.2670	0.77	3.5888	1.42	0.09750	1.19	0.80	1525	32	1547	32	1577	32	3
47.D	120.6	1.13	48.4	0.0025	0.3193	0.56	4.8845	1.22	0.11093	1.08	0.80	1787	36	1800	37	1815	37	2
48.D	95.5	0.48	44.2	0.0014	0.4159	0.57	8.1466	1.00	0.14206	0.82	0.80	2242	45	2247	45	2252	45	0
49.D	68.1	0.62	31.5	0.0015	0.4031	0.65	7.6360	1.16	0.13740	0.96	0.80	2183	44	2189	44	2195	44	1
51.D	40.2	0.70	14.4	0.0012	0.3125	0.78	4.6580	1.73	0.10810	1.55	0.80	1753	36	1760	37	1768	37	1
52.D	47.5	0.60	21.7	0.0030	0.4011	0.71	7.6107	1.39	0.13762	1.19	0.80	2174	44	2186	44	2197	44	1
53.D	62.2	0.88	17.2	0.0000	0.2337	0.82	2.7535	1.84	0.08546	1.64	0.80	1354	28	1343	30	1326	29	-2
54.D	125.1	3.24	87.6	0.0034	0.3843	0.58	6.9955	1.01	0.13201	0.82	0.80	2096	42	2111	42	2125	42	1
55.D	65.0	0.43	16.6	0.0000	0.2409	0.71	2.8241	1.64	0.08503	1.48	0.80	1391	29	1362	29	1316	28	-6
56.D	102.1	0.67	23.9	0.0009	0.2093	0.87	2.3623	1.65	0.08185	1.40	0.80	1225	26	1231	27	1242	26	1
57.D	242.2	1.41	126.4	0.0000	0.3869	0.74	6.9091	1.36	0.12952	1.14	0.80	2108	43	2100	43	2091	42	-1
58.D	38.7	1.03	7.3	0.0000	0.1566	0.78	1.5016	2.83	0.06956	2.72	0.77	938	20	931	25	916	24	-2
59.D	323.0	0.32	91.5	0.0006	0.2736	0.60	3.6611	0.99	0.09704	0.79	0.80	1559	32	1563	31	1568	31	1
60.D	457.4	0.65	110.1	0.0000	0.2158	0.53	2.4502	0.96	0.08233	0.79	0.79	1260	25	1257	25	1253	25	-1
61.D	177.9	0.55	65.2	0.0019	0.3306	0.56	5.1913	0.96	0.11389	0.78	0.80	1841	37	1851	37	1862	37	1
62.D	83.4	0.63	25.1	0.0017	0.2704	0.63	3.6170	1.45	0.09700	1.31	0.80	1543	31	1553	32	1567	32	2
63.D	70.9	0.49	15.5	0.0027	0.2043	0.70	2.3116	1.97	0.08208	1.84	0.80	1198	25	1216	27	1247	28	4
64.D	56.1	0.36	15.8	0.0016	0.2688	0.74	3.5762	1.60	0.09647	1.41	0.80	1535	32	1544	33	1557	32	1
66.D	536.9	0.68	67.9	0.0054	0.1147	0.69	1.0605	1.21	0.06706	0.99	0.80	700	14	734	16	839	17	17
67.D	314.1	0.27	85.3	0.0017	0.2666	0.53	3.5297	0.97	0.09602	0.81	0.79	1524	31	1534	31	1548	31	2
68.D	52.3	0.62	10.0	0.0000	0.1733	0.91	1.7466	2.50	0.07308	2.33	0.77	1030	22	1026	26	1016	25	-1
69.D	101.7	0.53	18.4	0.0024	0.1689	0.57	1.7363	1.68	0.07457	1.58	0.80	1006	20	1022	23	1057	23	5
70.D	360.0	0.59	85.7	0.0000	0.2174	0.46	2.4640	0.94	0.08218	0.82	0.79	1268	25	1262	26	1250	25	-1
71.D	147.62	0.16	36.43	0.0026	0.2511	0.97	3.2272	1.40	0.09321	1.01	0.79	1444	31	1464	31	1492	30	3

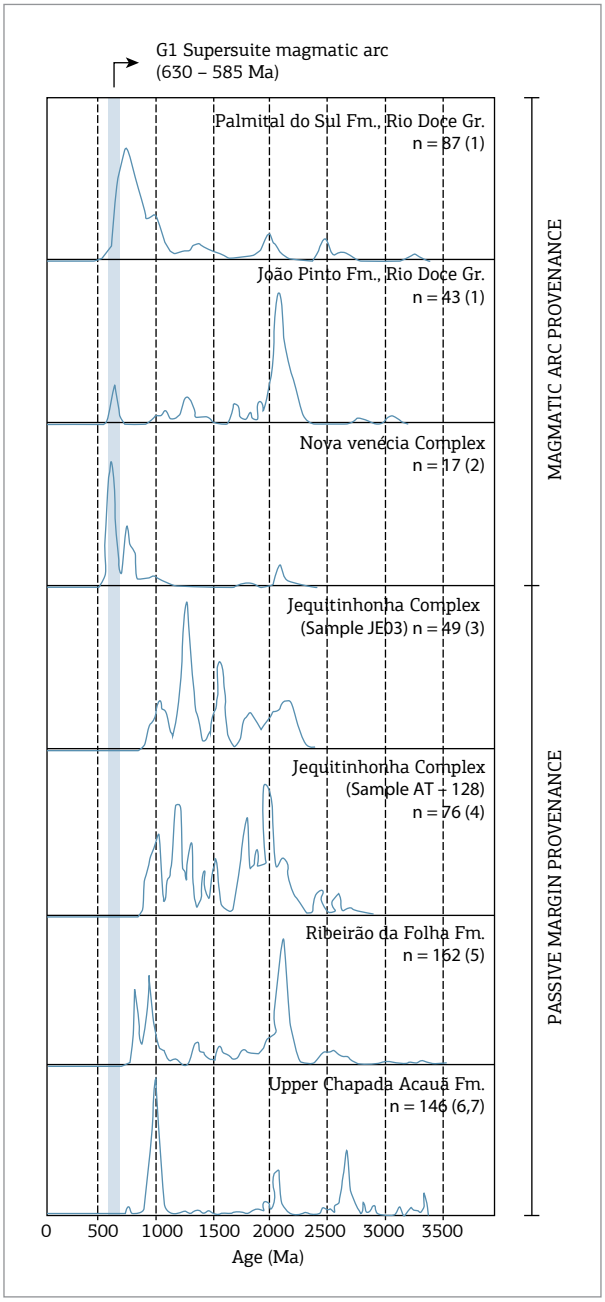

Figure 11. Detrital zircon age spectra of samples from the Jequitinhonha Complex in comparison to samples from the upper Macaúbas Group (passive margin) and the Rio Doce Group and Nova Venécia Complex (syn-orogenic arc-related basins). From: (1) Novo (2013); (2) Gradim *et al.* (2014); (3) this work; (4) Gonçalves-Dias *et al.* (2011); (5) Peixoto *et al.* (2015); (6) Pedrosa-Soares *et al.* (2000); (7) Kuchenbecker *et al.* (2015).

depositional age at about 900 Ma, and the main epoch of the syn-collisional metamorphism and anatexis suggests a minimum depositional age around 575 Ma (Siga Jr. *et al.* 1987, Pedrosa-Soares *et al.* 2011a, Silva *et al.* 2011, Gradim *et al.* 2014).

Discussion of the Sm-Nd data

The Nd evolution diagram for the paragneiss samples (Fig. 12) shows a comparison with the main possible sources as suggested by the U-Pb data from detrital zircon grains, that is, the Archaean-Palaeoproterozoic basement of the São Francisco craton and the Tonian rift-related volcanic rocks (Fig. 13; data from Teixeira *et al.* 1996, Noce *et al.* 2000, Tack *et al.* 2001). The positioning of the Jequitinhonha Complex samples in between the São Francisco craton and West Congo rift volcanics fields (Fig. 12A) suggests variable mixing between these two broad source areas as the main sedimentary provenance for the Jequitinhonha Complex protholits. The εNd evolution diagram also suggests an important role for the Tonian rift-related magmatism in the isotopic inheritance of the clay-rich protoliths such as those represented by the peraluminous gneiss of the distal Jequitinhonha Complex.

In comparison to the Jequitinhonha Complex, Nd isotope data for the Macaúbas Group metasedimentary and metavolcanic rocks shows a broader variation, with $\varepsilon Nd_{(575\ Ma)}$ from -2.0 (basic metavolcanics) to -18.0 (metasedimentary rocks) and T_{DM} model ages from 1.5 to 2.5 Ga (Babinski *et al.* 2012). Nevertheless, the homogeneous results found for the Jequitinhonha Complex plot within the range of samples from the Macaúbas Group in the Nd isotope evolution diagram (Fig. 12B).

Tectonic setting of the Jequitinhonha Complex and stratigraphic correlations

In the eastern portion of the Araçuaí orogen, medium- to high-grade metamorphic rocks whose sedimentary protoliths were deposited in syn-orogenic basins related to the G1 supersuite magmatic arc are quite common (Pedrosa-Soares *et al.* 2011a). This is the case of the Rio Doce Group (Nalini *et al.* 2000, Pedrosa-Soares *et al.* 2001, 2011b, Martins *et al.* 2004, Vieira 2007, Paes *et al.* 2010, Silva *et al.* 2011, Novo 2013) and the Nova Venécia Complex, composed of peraluminous paragneiss with intercalations of calcsilicate rocks (Noce *et al.* 2004, Pedrosa-Soares *et al.* 2008, Gradim *et al.* 2014). Both of those units bear an important detrital zircon U-Pb age peak at ca. 630 Ma, indicating provenance from the Araçuaí orogen magmatic arc. The Jequitinhonha Complex, on the other hand, yielded no Ediacaran zircons, but, instead, shows patterns which are more similar to the precursor passive margin basin of the orogen (upper Macaúbas Group), with younger zircons at around 900 Ma.

Thus, the above petrographic, litochemical, isotopic, and geochronologic data suggests that the Jequitinhonha Complex represents a sedimentary package deposited in a passive margin environment of the precursor basin of the Araçuaí orogen, between ca. 914 Ma (youngest peak from detrital zircon ages) and 580–540 Ma (age of the

syn-collisional metamorphism; Pedrosa Soares *et al.* 2011a). The Jequitinhonha Complex is then not correlative with other paragneiss successions of the eastern Araçuaí orogen, such as the Nova Venécia Complex, which is related to the back-arc region of the G1 supersuite magmatic arc (Fig. 2) (Noce *et al.* 2004), but, instead, probably represents a higher metamorphic grade chronostratigraphic equivalent of the upper units of the Macaúbas Group (Ribeirão da Folha and upper Chapada Acauã formations; Pedrosa-Soares *et al.* 2011b, Babinski *et al.* 2012, Kuchenbecker *et al.* 2015) with both series representing sand-mud shelf deposits. This is supported by trace element data of paragneiss samples, which suggest a trailing-edge environment of deposition, and by the very similar U-Pb detrital zircon age spectra and Sm-Nd isotope data for the Jequitinhonha and Macaúbas units.

The exclusively sedimentary nature of the Jequitinhonha Complex and the absence of any ophiolite slivers in the region reinforce the interpretation that it represents the ensialic part

Table 3. Nd isotopic data for rocks from the Jequitinhonha/Almenara region. T_{DM} is calculated after DePaolo's (1981) model.

Sample	Rock	Nd (ppm)	Sm (ppm)	$^{147}Sm/^{144}Nd$	$^{143}Nd/^{144}Nd$	Error (2σ)	$\varepsilon Nd_{(575\ Ma)}$	T_{DM} (Ga)
AL16B	paragneiss	48.14	8.87	0.11144	0.511961	0.000012	-7.0	1.6
RP64	paragneiss	33.19	6.18	0.11247	0.511914	0.000013	-8.0	1.7
AL21	paragneiss	33.35	6.36	0.1154	0.511946	0.000012	-7.6	1.7
AL01	paragneiss	37.59	7.45	0.11981	0.511980	0.000017	-7.2	1.7
RP51	paragneiss	45.11	8.82	0.11817	0.511954	0.000013	-7.6	1.7
AL03	paragneiss	42.11	8.34	0.11972	0.511959	0.000008	-7.7	1.7
AL19	paragneiss	40.06	7.72	0.11654	0.511919	0.000011	-8.2	1.8
AL27	paragneiss	36.77	7.24	0.11907	0.511936	0.000010	-8.0	1.8
JE08	paragneiss	44.86	9.11	0.12273	0.511956	0.000011	-7.9	1.8
AT-128	quartzite	5.19	0.95	0.11099	0.511400	0.000014	-17.9	2.4
RP64	duplicate	34.73	6.43	0.11184	0.511908	0.000008	-8.1	1.7
RP51	duplicate	41.37	8.06	0.11782	0.511940	0.000053	-7.9	1.7
BHVO-2	USGS standard	24.55	6.10	0.15017	0.512976	0.000008		

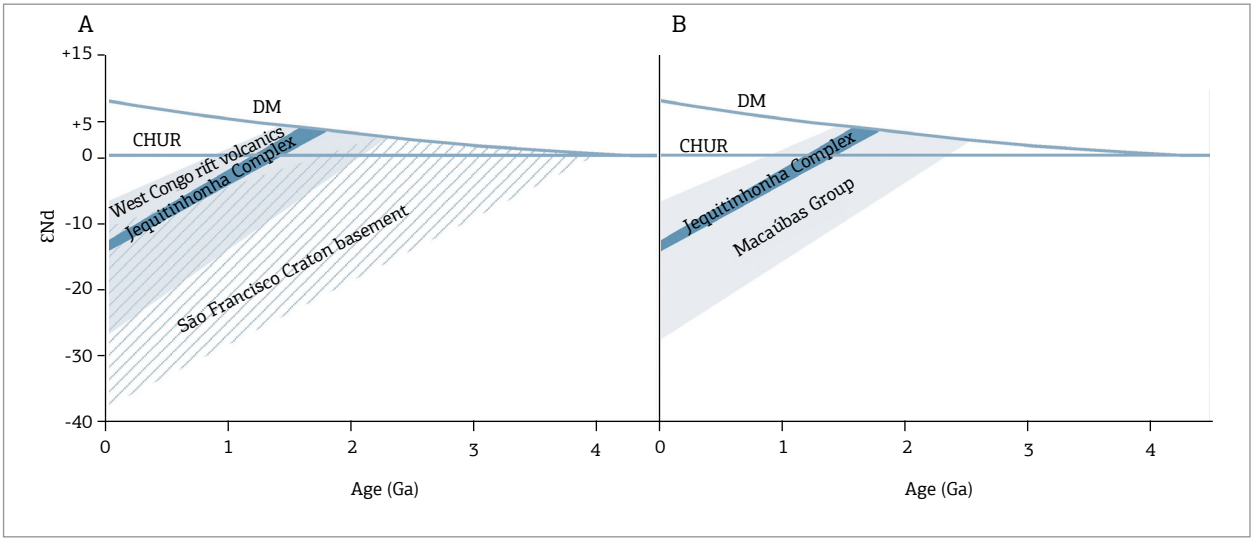

Figure 12. Nd isotopic evolution diagram for paragneiss samples of the Jequitinhonha Complex, as compared with (a) the São Francisco Craton basement (Teixeira *et al.* 1996, Noce *et al.* 2000) and Tonian rift volcanics of the West Congo belt (Tack *et al.* 2001); and (b) Macaúbas Group samples (Babinski *et al.* 2012).

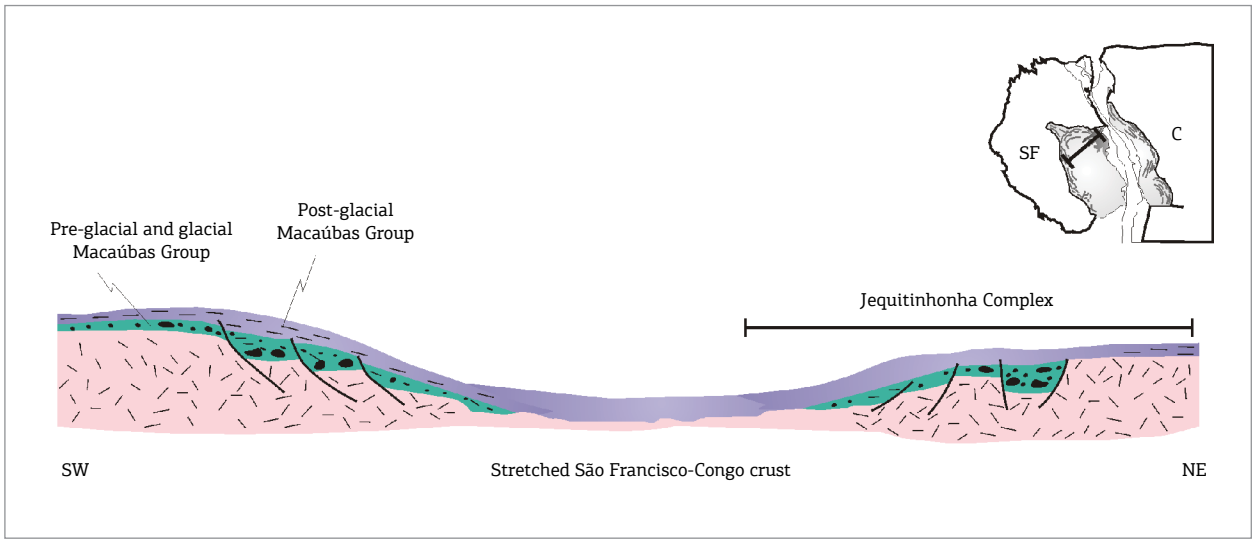

Figure 13. Tectonic model for the precursor basin of the Jequitinhonha Complex and its relations to the Macaúbas Group.

of the precursor gulf-like basin of the Araçuaí-West Congo orogen (Fig. 13). This scenario also supports the suggestion that the São Francisco-Congo paleocontinent was not broken to the north of the studied region as a consequence of the opening of the Macaúbas-Jequitinhonha basin. This interpretation provides further evidence that the São Francisco-Congo paleocontinent acted as a single plate during West Gondwana amalgamation in Ediacaran time, joined by the Bahia – Gabon cratonic bridge, as shown by virtually all paleogeographic reconstructions (e.g. Cordani *et al.* 2003, D'Agrella *et al.* 2004, Li *et al.* 2008).

CONCLUSIONS

1. Trace and REE element patterns of the Jequitinhonha Complex suggest erosion of an evolved continental crust, similar to present-day passive margin (trailing edge) turbidites, and are very different from present-day active margin (arc-related) basins.
2. The detrital zircon U-Pb age spectra of two quartzite samples indicates main source areas of ca. 1.0, 1.2, 1.5, and 2.2 Ga. The absence of Ediacaran zircon excludes, in principle, the Araçuaí orogen magmatic arc (G1 supersuite) as a probable source area. On the other hand, the detrital zircon age patterns of the Jequitinhonha Complex samples are very similar to those of the upper units of the Macaúbas Group (the upper Chapada Acauã and Ribeirão da Folha formations). The main suggested source areas are the São Francisco craton basement and the extensive Tonian bimodal volcanic units of the West Congo belt.
3. Sm-Nd isotope data on samples from the Jequitinhonha Complex are homogeneous, and suggest a mixing of detritus from Paleoproterozoic to Neoproterozoic crust of the source areas. As suggested by the U-Pb age spectra, the São Francisco craton basement and the Tonian rift volcanics of the West Congo belt are the two possible end-members of this mixing process. The Sm-Nd isotope data of the Jequitinhonha Complex is also coherent with an interpretation that it represents a distal chronostratigraphic equivalent of the upper Macaúbas Group, as samples from the Jequitinhonha Complex plot within the field of samples from the Macaúbas Group in a Nd isotope evolution diagram.
4. The Jequitinhonha Complex can be interpreted as part of the Neoproterozoic distal passive margin of the precursor basin to the Araçuaí orogen, with sedimentation of the protoliths probably during the Cryogenian. Thus, it is not related to other paragneiss units of the eastern Araçuaí orogen, such as the Nova Venécia Complex, whose protoliths were deposited in an arc-related basin ca. 635 Ma ago.

ACKNOWLEDGEMENTS

Our gratitude to the Brazilian scientific research agencies (CAPES, CNPq, FAPEMIG) and the Geological Survey of Brazil (CPRM) for the financial support. Tatiana Gonçalves Dias and Fabrício Caxito were supported by the ELAP (Emerging Leaders in the Americas Program) of the Canadian Bureau for International Education, and the Merit Scholarship Program of the Ministère de l'Education, du Loisir et du Sports du Québec (MELS), during their stay at the GEOTOP/UQAM, Montréal, Canada. The original manuscript was greatly improved after comments and suggestions by S.O. Verdecchia, R.J. Pankhurst and an anonymous reviewer.

REFERENCES

Alkmim F.F., Marshak S., Pedrosa-Soares A.C., Cruz S., Peres G.G., Cruz S.C.P., Whittington A. 2006. Kinematic evolution of the Araçuaí-West Congo orogen in Brazil and Africa: Nutcracker tectonics during the Neoproterozoic assembly of Gondwana. *Precambrian Research*, **149:**43-64.

Almeida F.F.M. 1977. O Cráton do São Francisco. *Revista Brasileira de Geociências*, **7**: 349-364.

Almeida F.F.M. & Litwinski N. 1984. Província Mantiqueira: setor setentrional. *In*: Almeida F.F.M. & Hasui Y. (eds.) *O Pré-Cambriano do Brasil*. São Paulo, Editora Edgar Blücher, p. 282-307.

Babinski M., Pedrosa-Soares A.C., Trindade R.I.F. Martins M., Noce C.M., Liu D. 2012. Neoproterozoic glacial deposits from the Araçuaí orogen, Brazil: Age, provenance and correlations with the São Francisco craton and West Congo belt. *Gondwana Research*, **21**(2-3):451-465.

Barbosa J.S.F. & Sabaté P. 2004. Archean and Paleoproterozoic crust of the São Francisco Craton, Bahia, Brazil: geodynamic features. *Precambrian Research*, **133**:1-27.

Belém J. 2006. *Caracterização mineralógica, física e termobarométrica de minérios de grafita da Província Grafítica Bahia-Minas*. Dissertação de Mestrado, Instituto de Geociências, Universidade Federal de Minas Gerais, 165 p.

Brito Neves B.B., Campos Neto M.C., Fuck R.A. 1999. From Rodinia to Western Gondwana: An approach to the Brasiliano-Pan African Cycle and orogenic collage. *Episodes*, **22**(3):155-166.

Caxito F.A., Uhlein A., Dantas E.L., Stevenson R., Pedrosa-Soares A.C. 2015. Orosirian (ca. 1.96 Ga) mafic crust of the northwestern São Francisco Craton margin: Petrography, geochemistry and geochronology of amphibolites from the Rio Preto fold belt basement, NE Brazil. *Journal of South American Earth Sciences*, **59**:95-111.

Celino J.J. 1999. *Variação composicional em suítes de granitóides neoproterozóicos e sua implicação na evolução do Orógeno Araçuaí (Brasil) – Oeste Congolês (África)*. Tese de Doutorado, Instituto de Geociências, Universidade de Brasília.

Chemale Jr. F., Dussin I.A., Alkmim F.F., Martins M.S., Queiroga G., Armstrong R., Santos M.N. 2012. Unravelling a Proterozoic basin history through detrital zircon geochronology: The case of the Espinhaço Supergroup, Minas Gerais, Brazil. *Gondwana Research*, **22**(1):200-206.

Cordani U.G., Brito Neves B.B., D'Agrella M.S., Trindade, R.I.F. 2003. Tearing-up Rodinia: the Neoproterozoic paleogeography of South American cratonic fragments. *Terra Nova*, **15**:343-349.

Daconti B.C. 2004. *Contexto geológico, controle e correlação regional das mineralizações de grafita da região de Almenara, Província Grafítica do Nordeste de Minas Gerais.* Dissertação de Mestrado, Instituto de Geociências, Universidade Federal de Minas Gerais.

Danderfer A., de Waele B., Pedreira A. J., Nalini Jr. H.A. 2009. New geochronological constraints on the geological evolution of Espinhaço basin within the São Francisco craton - Brazil. *Precambrian Research*, **170**:116-128.

D'Agrella-Filho M.S., Pacca I.G., Trindade R.I.F., Teixeira W., Raposo M.I.B., Onstott T.C. 2004. Paleomagnetism and $^{40}Ar/^{39}Ar$ ages of mafic dykes from Salvador (Brazil): new constraints on the São Francisco craton APW path between 1080 and 1010 Ma. *Precambrian Research*, **132**:55-77.

DePaolo D.J. 1981. Neodymium isotopes in the Colorado front range and crust-mantle evolution in the Proterozoic. *Nature*, **291**:193-196.

Drumond J.B.V. & Malouf R.F. 2010. *Carta Geológica, 1:100.000. Folha SE-24-V-A-III - Almenara.* Projeto Jequitinhonha, Programa Geologia do Brasil, CPRM.

Evans J.A., Stone P., Floyd J.D. 1991. Isotopic characteristics of Ordovician greywacke provenance in the Southern Uplands of Scotland. *In*: Morton A.C., Todd S.P., Haughton P.D.W. (eds.). *Developments in sedimentary provenance studies*. Geological Society Special Publication **57**:161-172.

Faure G. 1986. *Principles of Isotope Geology*. 2nd Edition. New York, John Wiley & Sons, 589 p.

Frost C.D. & Winston D. 1987. Nd isotopic systematic of coarse- and fine-grained sediments: examples from the Middle Proterozoic Belt Purcell Super Group. *Journal of Geology*, **95**:309-327.

Gomes A.C.B. 2010. *Carta Geológica, 1:100.000. Folha SE-24-V-A-VI – Rio do Prado.* Projeto Jequitinhonha, Programa Geologia do Brasil, CPRM.

Gonçalves-Dias T., Pedrosa-Soares A.C., Dussin I.A., Alkmim F.F., Caxito F.A., Silva L.C., Noce C.M. 2011. Idade máxima de sedimentação e proveniência do Complexo Jequitinhonha na área-tipo (Orógeno Araçuaí): primeiros dados U–Pb (LA-ICP-MS) de grãos detríticos de zircão. *Geonomos*, **19**(2):121-130.

Gradim C., Roncato J., Pedrosa-Soares A.C., Cordani U.G., Dussin I.A., Alkmim F.F., Queiroga G., Jacobsohn T., Silva L.C., Babinski M. 2014. The hot back-arc zone of the Araçuaí orogen, Eastern Brazil: from sedimentation to granite generation. *Brazilian Journal of Geology*, **44**(1):155-180.

Grommet L.P., Dymek R.F., Haskin L.A., Korotev R.L. 1984. The "North American shale composite": Its composition, major and trace element characteristics. *Geochimica et Cosmochimica Acta*, **48:**2469-2482.

Junqueira P.A., Gomes A.C.B., Raposo F.O, Paes V.J.C. 2010. *Carta Geológica, 1:100.000. Folha SE-24-V-A-V – Joaíma.* Projeto Jequitinhonha, Programa Geologia do Brasil, CPRM.

Kuchenbecker M., Pedrosa-Soares A.C., Babinski M., Fanning M. 2015. Detrital zircon age patterns and provenance assessment for pre-glacial to post-glacial successions of the Neoproterozoic Macaúbas Group, Araçuaí orogen, Brazil. *Precambrian Research*, **266**:12-26.

Li Z.X., Bogdanova S.V., Collins A.S., Davidson A., de Waele B., Ernst R.E., Fitzsimons I.C.W., Fuck R.A., Gladkochub D.P., Jacobs J., Karlstrom K.E., Lu S., Natapov L.M., Pease V., Pisarevsky S.A., Thrane K., Vernikovsky V. 2008. Assembly, configuration, and break-up history of Rodinia: A synthesis. *Precambrian Research*, **160:**179-210.

Ludwig K.R. 2008. *User's manual for Isoplot 3.6. A geochronological toolkit for Microsoft Excel*. Berkeley Geochronologic Center, Special Publication No. 4, Berkeley, USA.

Machado N., Schrank A., Abreu F.R., Knauer L.G., Almeida-Abreu P.A. 1989. Resultados preliminares da geocronologia U/Pb na Serra do Espinhaço Meridional. *In*: SBG, Simpósio de Geologia de Minas Gerais, 5, *Anais*, p. 1-4.

Martins V.T.S., Teixeira W., Noce C.M., Pedrosa-Soares A.C. 2004. Sr and Nd characteristics of Brasiliano-Pan African granitoid plutons of the Araçuaí orogen, southeastern Brazil: Tectonic implications. *Gondwana Research*, **7**:75-89.

McLennan S.M., Taylor S.R., McCulloch M.T., Maynard J.B. 1990. Geochemical and Nd-Sr isotopic composition of deep-sea turbidites: Crustal evolution and plate tectonic associations. *Geochimica et Cosmochimica Acta*, **54**:2015-2050.

Mehnert K.R. 1971. *Migmatites and the Origin of Granitic Rocks*. Amsterdan, Elsevier, 405 pp.

Moraes R., Nicollet C., Barbosa J.H.F., Fuck R.A., Sampaio A.R. 2015. Applications and limitations of thermobarometry in migmatites and granulites using as an example rocks of the Araçuaí Orogen in southern Bahia, including a discussion on the tectonic meaning of the current results. *Brazilian Journal of Geology*, **45**(4):517-539.

Nalini Jr. H.A., Bilal E., Neves J.M.C. 2000. Syn-collisional peraluminous magmatism in the Rio Doce region: mineralogy, geochemistry, and isotopic data of the Neoproterozoic Urucum Suite (eastern Minas Gerais State, Brazil). *Revista Brasileira de Geociências*, **30:**120-125.

Noce C.M., Macambira M.B., Pedrosa-Soares A.C. 2000. Chronology of Neoproterozoic-Cambrian granitic magmatism in the Araçuaí Belt, Eastern Brazil, based on single zircon evaporation dating. *Revista Brasileira de Geociências*, **30**:25-29.

Noce C.M, Pedrosa-Soares A.C., Piuzana D., Armstrong R., Laux J.H., Campos C.M., Medeiros S.R. 2004. Ages of sedimentation of the kinzigitic complex and of a late orogenic thermal episode in the Araçuaí orogen, northern Espírito Santo State, Brazil: Zircon and monazite U-Pb SHRIMP and ID-TIMS data. *Revista Brasileira de Geociências*, **349**:587-592.

Noce C.M., Pedrosa-Soares A.C., Silva L.C., Alkmim F.F. 2007. O Embasamento Arqueano e Paleoproterozóico do Orógeno Araçuaí. *Geonomos*, **15**(1)**:**17-23.

Novo T.A. 2013. *Caracterização do Complexo Pocrane, magmatismo básico mesoproterozóico e unidades neoproterozóicas do sistema Araçuaí–Ribeira, com ênfase em geocronologia U-Pb (SHRIMP e LA–ICP–MS)*. Phd Thesis, Universidade Federal de Minas Gerais, Belo Horizonte, 193 p.

Paes V.J.C., Raposo F.O., Pinto C.P., Oliveira F.A.R. 2010. *Projeto Jequitinhonha, Estados de Minas Gerais e Bahia: texto explicativo. Geologia e Recursos Minerais das Folhas Comercinho, Jequitinhonha, Almenara, Itaobim, Joaíma e Rio do Prado*. Programa Geologia do Brasil. Belo Horizonte, CPRM, 376 p.

Pedrosa-Soares A.C., Noce C.M., Vidal P., Monteiro R., Leonardos O.H. 1992. Toward a new tectonic model for the Late Proterozoic Araçuaí (SE Brazil) - West Congolian (SW Africa) Belt. *Journal of South American Earth Sciences*, **6**:33-47.

Pedrosa-Soares A.C., Vidal P., Leonardos O.H., Brito-Neves B.B. 1998. Neoproterozoic oceanic remnants in eastern Brazil: Further evidence and refutation of an exclusively ensialic evolution for the Araçuaí-West Congo Orogen. *Geology*, **26**:519-522.

Pedrosa-Soares A.C., Cordani U.G., Nutman A. 2000. Constraining the age of Neo-proterozoic glaciation in eastern Brazil: first U-Pb (SHRIMP) data of detrital zircons. *Revista Brasileira de Geociências*, **30**:58-61.

Pedrosa-Soares A.C., Noce C.M., Wiedemann C.M., Pinto C.P. 2001. The Araçuaí–West Congo orogen in Brazil: An overview of a confined orogen formed during Gondwanland assembly. *Precambrian Research*, **110**:307-323.

Pedrosa-Soares A.C., Noce C.M., Alkmim F.F., Silva L.C., Babinski M., Cordani U., Castañeda C. 2007. Orógeno Araçuaí: Síntese do Conhecimento 30 anos após Almeida 1977. *Geonomos*, **15**(1):1-16.

Pedrosa-Soares A.C., Alkmim F.F., Tack L., Noce C.M., Babinski M., Silva L.C., Martins-Neto M.A. 2008. Similarities and differences between the Brazilian and African counterparts of Neoproterozoic Araçuaí-West Congo orogen. *In*: Pankhrust R., Trouw R., Brito-Neves B B., Wit M. (eds). *The Gondwana Peleocontinent in the South Atlantic Region*. Geological Society of London, Special Publications, **294**:153-172.

Pedrosa-Soares A.C., Campos C.P., Noce C., Silva L.C., Novo T., Roncato J., Medeiros S., Castañeda C., Queiroga G., Dantas E., Dussin I., Alkmim F.F. 2011a. Late Neoproterozoic-Cambrian granitic magmatism in the Araçuaí orogen (Brazil), the Eastern Brazilian Pegmatite Province and related mineral resources. *In:* Sial A.N., Bettencourt J.S., De Campos C.P., Ferreira V.P. (eds). *Granite-Related Ore Deposits*. Geological Society, London, Special Publications, **350**:25-51.

Pedrosa-Soares A.C., Babinski M., Noce C., Martins M., Queiroga G., Vilela F. 2011b. The Neoproterozoic Macaúbas Group (Araçuaí orogen, SE Brazil) with emphasis on the diamictite formations. *In*: Arnaud E., Halverson G., Shields G. (eds). *The Geological Record of Neoproterozoic Glaciations*. Geological Society of London, *Memoir* **36**, chapter 49.

Pedrosa-Soares A.C. & Alkmim F.F. 2011. How many rifting events preceded the development of the Araçuaí-West Congo orogen? *Geonomos*, **19**(2): 244-251.

Peixoto E.N., Pedrosa-Soares A.C., Alkmim F.F., Dussin I.A. 2015. A suture-related accretionary wedge formed in the Neoproterozoic Araçuaí orogen (SE Brazil) during Western Gondwanaland assembly. *Gondwana Research*, **27**:878-896.

Pinto C.P. 2010. *Carta Geológica, 1:100.000. Folha SE-24-V-A-II – Jequitinhonha*. Projeto Jequitinhonha, Programa Geologia do Brasil , CPRM.

Powell R. & Holland T. 1994. Optimal geothermometry and geobarometry. *American Mineralogist*, **79**:120-133.

Queiroga G.N., Pedrosa-Soares A.C., Noce C.M., Alkmim F.F., Pimentel M.M., Dantas E., Martins M., Castañeda C., Suita M.T.F., Prichard H. 2007. Age of the Ribeirão da Folha ophiolite, Araçuaí Orogen: The U-Pb zircon dating of a plagiogranite. *Geonomos*, **15**:61-65.

Reis L.B. 1999. *Estudos de mineralizações de grafita no extremo nordeste de Minas Gerais*. Dissertação de Mestrado, Instituto de Geociências, Universidade Federal de Minas Gerais, Minas Gerais.

Rosa M.L.S., Conceição H., Macambira M., Galarza M.C., Cunha M., Menezes R., Marinho M.M., Cruz-Filho B.E., Rios D.C. 2007. Neoproterozoic anorogenic magmatism in the Southern Bahia Alkaline Province of NE Brazil: U-Pb and Pb-Pb ages of the blue sodalite syenites. *Lithos*, **97**:88-97.

Siga Jr. O., Cordani U.G., Basei M.A.S., Teixeira W., Kawashita K., Van Schmus W.R. 1987. Contribuição ao estudo geológico e geocronológico da porção nordeste de Minas Gerais. *In*: 48º Simpósio de Geologia de Minas Gerais. SBG-MG, *Boletim*, **7**:29-44.

Silva L.C., Armstrong R., Noce C.M., Carneiro M., Pimentel M.M., Pedrosa-Soares A.C., Leite C., Vieira V.S., Silva M., Paes V., Cardoso-Filho J. 2002. Reavaliação da evolução geológica em terrenos pré-cambrianos brasileiros com base em novos dados U-Pb SHRIMP, parte II: Orógeno Araçuaí, Cinturão Móvel Mineiro e Cráton São Francisco Meridional. *Revista Brasileira de Geociências*, **32**:513-528.

Silva L.C, Pedrosa-Soares A.C., Teixeira L., Armstrong R. 2008. Tonian rift-related, A-type continental plutonism in the Araçuaí Orogen, eastern Brazil: New evidence for the breakup stage of the São Francisco Congo Paleocontinent. *Gondwana Research*, **13**:527-537.

Silva L.C., Pedrosa-Soares A.C., Armstrong R., Noce C.M. 2011. Determinando a duração do período colisional do Orógeno Araçuaí com base em geocronologia U-Pb de alta resolução em zircão: uma contribuição para a história da amalgamação do Gondwana Ocidental. *Geonomos*, **19**(2):180-197.

Tack L., Wingate M.T.D., Liégeois J.P., Fernandez-Alonso M., Deblond A. 2001. Early Neoproterozoic magmatism (1000-910 Ma) of the Zadinian and Mayumbian groups (Bas-Congo): Onset of Rodinian rifting at the western edge of the Congo craton. *Precambrian Research*, **110**:277-306.

Taylor S.R. & McLennan S.M. 1985. *The Continental Crust: Its Composition and Evolution*. Blackwell, Oxford.

Teixeira W., Carneiro M.A., Noce C.M., Machado N., Sato K., Taylor P.N. 1996. Pb, Sr and Nd isotope constraints on the Archaean evolution of gneissic-granitoid complexes in the southern São Francisco Craton, Brazil. *Precambrian Research*, **78:**151-164.

Teixeira W., Sabaté P., Barbosa J.S.F., Noce C.M., Carneiro M.A. 2000. Archean and Paleoproterozoic Tectonic evolution of the São Francisco Craton, Brazil. *In:* Cordani U.G., Milani E.J., Thomas Filho A., Campos D.A. (eds.). *Tectonic Evolution of the South America.* International Geological Congress, 31, Rio de Janeiro, Brazil, p. 101-137.

Teixeira L.R. 2002. *Relatório Temático de Litogeoquímica. Projeto Extremo Sul da Bahia*. 2002. Programa de Levantamentos Geológicos Básicos do Brasil. CPRM/CBPM.

Thiéblemont D., Prian J.P., Goujou J.C., Boulingui B., Ekogha H., Kassadou A.B., Simo-Ndounze S., Walemba A., Préat A., Theunissen K., Cocherie A., Guerrot C. 2011. Timing and characteristics of Neoproterozoic magmatism in SW-Gabon: First geochronogical and geochemical data on the West-Congolian orogen in Gabon (SYSMIN project, Gabon 2005-2009). *In:* 23 Colloquium of African Geology, *Posters and Abstracts*.

Trompette R.R. 1994. *Geology of Western Gondwana (2000-500 Ma). Pan-African-Brasiliano aggregation of South America and Africa.* A.A. Rotterdam, Balkema, 350 pp.

Uhlein A., Egydio-Silva M., Bouchez J.L., Vauchez A. 1998. The Rubim pluton (Minas Gerais, Brazil): a petrostructural and magnetic fabric study. *Journal of South American Earth Sciences*, **11**:179-189.

Vieira V.S. 2007. *Significado do Grupo Rio Doce no Contexto do Orógeno Araçuaí.* Tese de Doutorado, Instituto de Geociências, Universidade Federal de Minas Gerais, Belo Horizonte.

Available at www.sbgeo.org.br